

OPTIMAL AND IMPLEMENTABLE TRANSMISSION SCHEMES FOR ENERGY
HARVESTING NETWORKS

A THESIS SUBMITTED TO
THE GRADUATE SCHOOL OF NATURAL AND APPLIED SCIENCES
OF
MIDDLE EAST TECHNICAL UNIVERSITY

BY

FATİH MEHMET ÖZÇELİK

IN PARTIAL FULFILLMENT OF THE REQUIREMENTS
FOR
THE DEGREE OF MASTER OF SCIENCE
IN
ELECTRICAL AND ELECTRONICS ENGINEERING

SEPTEMBER 2012

Approval of the thesis:

**OPTIMAL AND IMPLEMENTABLE TRANSMISSION SCHEMES FOR ENERGY
HARVESTING NETWORKS**

submitted by **FATİH MEHMET ÖZÇELİK** in partial fulfillment of the requirements for the degree of **Master of Science in Electrical and Electronics Engineering Department, Middle East Technical University** by,

Prof. Dr. Canan Özgen
Dean, Graduate School of **Natural and Applied Sciences** _____

Prof. Dr. İsmet Erkmen
Head of Department, **Electrical and Electronics Engineering** _____

Assoc. Prof. Dr. Elif Uysal-Bıyıkoğlu
Supervisor, **Electrical and Electronics Engineering Dept., METU** _____

Examining Committee Members:

Prof. Dr. Yalçın Tanık
Electrical and Electronics Engineering Dept., METU _____

Assoc. Prof. Dr. Elif Uysal-Bıyıkoğlu
Electrical and Electronics Engineering Dept., METU _____

Assoc. Prof. Dr. Ali Özgür Yılmaz
Electrical and Electronics Engineering Dept., METU _____

Assist. Prof. Dr. Tolga Girici
Electrical and Electronics Engineering Dept., TOBB ETU _____

Tuğcan Aktaş, M.Sc.
Electrical and Electronics Engineering Dept., METU _____

Date: _____

I hereby declare that all information in this document has been obtained and presented in accordance with academic rules and ethical conduct. I also declare that, as required by these rules and conduct, I have fully cited and referenced all material and results that are not original to this work.

Name, Last Name: FATİH MEHMET ÖZÇELİK

Signature :

ABSTRACT

OPTIMAL AND IMPLEMENTABLE TRANSMISSION SCHEMES FOR ENERGY HARVESTING NETWORKS

Özçelik, Fatih Mehmet

M.S., Department of Electrical and Electronics Engineering

Supervisor : Assoc. Prof. Dr. Elif Uysal-Bıyıkoğlu

September 2012, 81 pages

Progress in energy harvesting technology and the increasing need for the energy efficient and environmentally friendly applications have called for reconsideration of communication systems. This reconsideration results in new problem formulations regarding the recent developments on energy harvesting systems. Recently, optimal strategies for various types of energy harvesting networks have been developed based on different harvesting models. This thesis reports the results of our research to develop the optimal scheduling structures on an energy harvesting broadcast and fading channels, and to devise online implementable algorithms for a point-to-point communication system. Particularly, structural properties of an optimal offline schedule in, (1) an energy harvesting broadcast channel with one transmitter two receivers, (2) a single user communication system under fading conditions, are investigated. Moreover, an online algorithm is proposed for a single-user energy harvesting communication system considering the physical constraints and necessities regarding implementation. The proposed scheme is implemented through GNU Radio framework on a USRP device.

Keywords: wireless communication, packet scheduling, energy harvesting, energy-efficient

communication, implementation

ÖZ

ENERJİ HARMANLAYAN AĞLAR İÇİN OPTİMUM VE GERÇEKLENEBİLİR İLETİM ŞEMALARI

Özçelik, Fatih Mehmet

Yüksek Lisans, Elektrik ve Elektronik Mühendisliği Bölümü

Tez Yöneticisi : Doç. Dr. Elif Uysal-Bıykoğlu

Eylül 2012, 81 sayfa

Enerji harmanlama teknolojisinde yaşanan gelişmeler, enerji verimli ve çevre dostu uygulamalara duyulan ihtiyacın giderek artması, haberleşme sistemleri tasarımının yeniden gözden geçirilmesi konusunu gündeme getirmiştir. Enerji harmanlayan sistemlerdeki güncel gelişmeler ışığında, yeni problem tanılamaları geliştirilmiştir. Son dönemde, çeşitli ağlar için farklı enerji harmanlama modelleri geliştirilerek, optimum çözümler araştırılmıştır. Bu tez kapsamında yürütülen çalışmalar, enerji harmanlayan gönderici için yayın ve sönümleme kanalları üzerinde en iyi çizelgeleme yapısını araştırmaya ve enerji harmanlayan noktadan-noktaya bir haberleşme sistemi için gerçekleştirilebilir algoritmalar üretmeye yöneliktir. Özellikle, enerji harmanlayarak, (1) iki kullanıcı bir yayın, (2) tek kullanıcı sönümleme kanalları üzerinde iletim yapan göndericilerin sahip olması gereken optimum çizelgeleme yapısı araştırılmıştır. Bununla birlikte, tek kullanıcı bir haberleşme sistemi için uygulamaya yönelik gereksinimler ve fiziksel kısıtlar göz önünde bulundurularak bir çizelgeleme algoritması öne sürülmüştür. Söz konusu iletim yapısı GNU Radio geliştirme platformu aracılığıyla, bir USRP cihazı üzerinde gerçekleştirilmiştir.

Anahtar Kelimeler: kablosuz haberleşme, paket çizelgeleme, enerji harmanlama, enerji verimli haberleşme, gerçekleştirme

To my beloved family

ACKNOWLEDGMENTS

Throughout the course of this study, I have had the opportunity to interact with a wide range of people. Even though I cannot express my gratitude to each of them individually, I would like to acknowledge some that particularly helped and motivated this research.

My supervisor Professor Elif Uysal-Bıyıkođlu has supported and inspired the research from its inception and it would not be possible to complete this thesis without her guidance and encouragement. Her wise supervision on this study from academical and technical aspects made this dissertation possible and helped me find my way on the career path. I am very grateful for her interest in this work and appreciate the kindness and friendly attitude during the whole period of time.

It has been my fortune to collaborate with Hakan Erkal, Göksele Uçtu, Baran Tan Bacinođlu and Neyre Tekbıyık. I wish to thank them all for the useful discussion along with the contributions to this study and me personally. I would like to thank to my colleagues, in addition, for their moral support, friendship and lively discussions.

I am very grateful to my close friends for their supportive attitudes. Specially, their company has been my breathing space during distressing times. Although I will not take the risk to leave someone out by pronouncing the names, I am sure they will find the wholehearted thoughts within these lines.

My most heart felt gratitude goes to my family. Their support, patience and, most importantly, love have encouraged me all the time. I will always be in depth for their parenthood and accompany.

I would like to acknowledge Türk Telekom Group for their support and collaboration during this study.

Lastly, I would like to acknowledge the Scientific and Technological Research Council of Turkey (TÜBİTAK) for the support they have provided during the course of my graduate education.

TABLE OF CONTENTS

ABSTRACT	iv
ÖZ	vi
ACKNOWLEDGMENTS	ix
TABLE OF CONTENTS	x
LIST OF TABLES	xii
LIST OF FIGURES	xiii
CHAPTERS	
1 INTRODUCTION	1
2 LITERATURE REVIEW	3
2.1 Information Theoretic Analysis	4
2.2 Resource Allocation Problems	5
2.3 Implementation Oriented Studies	8
3 OPTIMAL OFFLINE ALGORITHMS	10
3.1 Offline Broadcast Channel Problem	11
3.1.1 System Model	12
3.1.2 Structure of an Optimal Policy	16
3.1.3 Solution of Offline Broadcast Problem	18
3.2 Single User Offline Fading Channel Problem	19
3.2.1 System Model	20
3.2.2 An Equivalent Problem	22
3.2.3 Solution of Problem 3	23
3.2.4 Solution of Problem 2	25
3.2.5 Computational Complexity	26
3.2.6 Numerical Results	27

4	AN IMPLEMENTABLE ALGORITHM: TriMod	30
4.1	Implementability Concerns	31
4.1.1	Discrete Set of Data Rates	32
4.1.2	Power Amplifiers	32
4.1.3	Adaptation to Channel State	33
4.1.4	Energy Storage	34
4.1.5	Harvesting	35
4.1.6	Temporal Scaling	35
4.1.7	Complexity	36
4.2	Energy Conservation Intuitions	36
4.2.1	Transmit Power Reduction	37
4.2.2	Avoidance of Idleness	37
4.2.3	Channel Adaptation	38
4.2.4	Battery Adjustment	38
4.3	The Algorithm	39
4.4	IEEE 802.11	45
4.5	Optimal Offline Schedule	46
4.6	Numerical Study	48
4.7	Implementation Experiment	57
4.7.1	GNU Radio	58
4.7.2	USRP	59
4.7.3	The Experiment	60
5	CONCLUSIONS	64
	REFERENCES	67
A	PROOF OF LEMMA 3.1.2	72
B	PROOF OF LEMMA 3.1.3	76
C	PROOF OF LEMMA 3.2.1	77
D	IMPLEMENTATION DETAILS	79

LIST OF TABLES

TABLES

Table 4.1	IEEE 802.11g data rates, modulation modes and coding rates	45
Table 4.2	A subset of 802.11g data rates, corresponding threshold and maximum throughput values	49
Table D.1	Test-equipment details	79

LIST OF FIGURES

FIGURES

Figure 2.1	The heliomote prototype node [5].	9
Figure 3.1	Two-user broadcast setting	11
Figure 3.2	Example for (a) a sequence of energy and data arrivals, (b)-(c) the corresponding $E(t), B(t)$, (d) the schedule $P(t)$ and $\{r_{1i}, r_{2i}\}$	13
Figure 3.3	An example sequence of events: $t_i, i \geq 1$ are event times (energy harvests marked as E_i , channel state changes, h_i , or data arrivals B_i). The ξ_i denote inter-event epoch durations.	21
Figure 3.4	(a) An example event sequence. The squared channel gain in the i^{th} epoch is h_i , the bandwidth is $W = 1$ KHz, energy harvest amounts and arriving data are marked as E_i and B_i , respectively. (b) Final schedule returned by completion time minimization algorithm.	28
Figure 3.5	(a) An example event sequence. The squared channel gain in the i^{th} epoch is h_i , the bandwidth is $W = 1$ KHz, energy harvest amounts and arriving data are marked as E_i and B_i , respectively. (b) Final schedule returned by completion time minimization algorithm.	29
Figure 4.1	Flow graph representation of the TriMod algorithm	43
Figure 4.2	TriMod vs RBAR for different data arrival rates. First set of data is obtained for the initial slot length values of 8 and 16 ms corresponding to generous and conservative modes, respectively. The second set of data is obtained under doubled initial slot length assignment for conservative and generous modes.	51

Figure 4.3 TriMod vs RBAR for different energy arrival rates. First set of data is obtained for the initial slot length values of 8 and 16 ms corresponding to generous and conservative modes, respectively. The second set of data is obtained under doubled initial slot length assignment for conservative and generous modes. . . .	52
Figure 4.4 TriMod vs RBAR for different initial battery levels. First set of data is obtained by varying initial battery levels of each policy, while the second is obtained by changing just the initial battery level of the transmitter where TriMod operates.	53
Figure 4.5 (a) Corresponding event setting used in the experiment. The squared channel gain in the i^{th} epoch is h_i , energy harvest amounts and arriving data are marked as E_i and B_i , respectively. (b) Power assignments in dBm. (c) Final rate schedule of the policies.	55
Figure 4.6 a) Corresponding event setting used in the experiment. The squared channel gain in the i^{th} epoch is h_i , energy harvest amounts and arriving data are marked as E_i and B_i , respectively. (b) Power assignments in dBm. (c) Final rate schedule of the policies.	56
Figure 4.7 A typical software radio structure	58
Figure 4.8 GNU Radio-Basic Architecture	59
Figure 4.9 Test bed platform used in implementation experiment	61
Figure 4.10 A screen view from the experimentation computer	63
Figure A.1 Illustration of the transmission scheme used in Lemma 3.1.2.	72

CHAPTER 1

INTRODUCTION

Ranging from the financial costs to emission and wasted resources, energy efficiency is the key to the solution of many problems. According to a comprehensive research by *International Energy Agency* [1], investments on conservation of energy by 2050 could save the world's energy consumption by one third. A significant part of this consideration, specially, involves dissipation of energy due to telecommunications ICT.

As in other fields, energy efficiency and lifetime maximization tasks are crucial in communication systems. Research in this field has drawn considerable interest in the last decade and there have been numerous studies investigating how to allocate the resources in a more efficient and economical way [2]-[37]. Together with the increasing number of battery powered wireless devices, conservation of energy has even become more important. Indeed, in today's world, many of the communication devices are supplied by batteries due to the mobility requirements. Expanding the operating and stand-by times of these devices, i.e., sensor nodes, mobile phones, tablet PC's etc., is an essential design consideration. To this end, harvesting ambient energy along with efficient energy usage techniques has been proposed as a rational settlement.

Energy harvesting communication systems involve transmitters being powered by environmental sources such as solar, vibration, and thermal effects, either alone or as supplement to the power drawn from a grid. The ability to supply the energy storage units from environmental sources can be very useful for distributed networks such as wireless sensor networks, M2M networks. Such networks are designed to work in the absence of a pre-established infrastructure. However, battery depletion of a single node might severely affect this structure and burden high maintenance costs into the system as a consequence. It has been shown in

several studies [2, 3, 4] that, scavenging environmental energy may result battery unlimited operation and resolve the issue. Recent developments in ambient energy harvesting technologies have already resulted in the practical implementation of such systems [5].

Dependence on a variable energy source poses interesting new challenges for the transmission of information. For example, allocation of resources solely based on current state of the system does not guarantee an effective solution. In addition to present circumstances, future events are also need to be taken into consideration in a causal way. Along with such concerns, in this thesis, we investigate optimal and implementable transmission schemes. Specifically, the thesis consists of two specific avenues of work. In the first part, optimal transmission strategies under two different communication settings, i.e., two-user broadcast and single user fading channels, are considered in an *offline* fashion. Based on the structured mathematical formulation, overall communication delay is aimed to be minimized. Firstly, structural properties of the optimal solution in the BC problem is studied. Next, fading channel problem is formulated and the solution is shown to be reachable through iterative runs of a convex optimization technique. The second part of the thesis focus on the development and employment of an implementable novel transmission strategy considering physical and practical concerns.

The thesis consists of 5 chapters. In the following chapter, recent developments in energy harvesting networks will be reviewed. Starting with the information theoretic bounds, resource management schemes will be featured. After that, implementation oriented studies will conclude the chapter.

In Chapter 3, two similar offline scheduling formulations will be analysed. Firstly, structure of the problem solution in [6] will be restudied. Afterwards, the focus will be moved to another communication setting by rearranging the formulation in [7] as a packet scheduling problem.

In Chapter 4, the focus will be moved to the practicality concerns and development of a low-complexity heuristic. Next, the conceived scheme will be numerically analysed by comparisons and it will be tested at a basic level on an experimental hardware/software test platform.

Finally, key points emphasized throughout the thesis will be summarized in Chapter 5 and possible future avenues of work will be discussed.

CHAPTER 2

LITERATURE REVIEW

Energy efficient and green wireless communication have become a major design consideration due to the growing concerns on environmental and operating costs raised by dramatically increasing communication devices [8, 9, 10]. In general, how to design an energy efficient and environmental friendly communication scheme depends largely on the power supply. In traditional communication systems, a connection to the fixed power grid or a rechargeable, replaceable battery provides the required energy to power up the device. Operation or lifetime of such systems is mostly limited by the power constraint or the battery size of the supply unit. Specially, in some networks, i.e., sensor networks, M2M networks, lifetime of the system is determined by the battery life of the units. As the replacement of batteries might be too costly, dangerous or even impossible in some cases, i.e., border surveillance, toxic environment and human-body monitoring applications, depletion of battery needs to be prevented or postponed as much as possible. To prolong operation time, several energy efficiency mechanisms, ranging from duty-cycle adaptation to energy efficient medium access and routing schemes, have been proposed [11, 12].

Recently, struggles in this field have focused on scavenging ambient energy so as to maximize operation time. Along with this idea, new design challenges have come onto the scene. Although replenishment of energy from environmental sources can contribute to achieve battery independent operation, energy harvesting may not guarantee a complete solution. Additional efforts to adapt and optimize the design parameters and the allocation of resources, which has drawn a great deal of attention from the research community [25]-[37], are required. Within this chapter, a short review of recent body literature will be presented. We start with information theoretic analysis of energy harvesting communication networks. Next, resource allocation problems, including offline scheduling schemes, will be reviewed. Finally, studies

regarding practical concerns and implementation will be summarized.

2.1 Information Theoretic Analysis

Capacity of a point-to-point energy harvesting communication system under AWGN is studied in [13] and [14]. It has been shown that, channel capacity in this case corresponds to the capacity of a single transmitter with an average power constraint equal to the constant recharge rate under ideal battery and AWGN conditions. In [13], two different proposed schemes, save-and-transmit and best-effort-transmit, have been proven to achieve the capacity. In addition, the link between throughput optimal and capacity achieving policies is shown in [14].

In addition to the transmission, there are some other sources of energy consumption, i.e., sensing, processing etc., in a communication device. In [14], capacity is also derived taking the energy consumption of sub-units into consideration. In this case, capacity is shown to match the capacity of a conventional AWGN transmitter with average power constraint equal to the recharge rate reduced by average processing power cost. Additionally, effects caused by imperfections of battery has also been computed in [14].

Next, Shannon capacity of an energy harvesting sensor node over a fading AWGN channel has been examined [15]. Starting the analysis with some ideal assumptions, i.e., infinite capacity battery, perfect channel state information (CSI), no storage inefficiency, capacity expression has been derived and results are extended to more realistic cases by relaxing the assumptions one by one. It has been shown that instantaneous water-filling achieves capacity. Furthermore, different harvest-store mechanisms have been compared under different buffer size and storage inefficiency conditions.

In a more realistic transmitter model, assumption of available data to transmit in all time shall also be relaxed. Combining queueing and information theoretic approaches, results in [13] and [14] have been extended in [16]. Deriving the necessary conditions to satisfy stability, capacity expression is obtained and it is shown how to obtain throughput optimal policies. Moreover, capacity formulation in [16] has also been considered under fading conditions and boundary of the achievable rate region is obtained.

Although single user capacity expressions provide intuitions into nature of the information

theoretical bound, network scale examination is necessary to understand the limits of energy harvesting communication systems. In [17], capacity analysis of recharge capable nodes under Gaussian multiple access channel is considered. Each node is thought to be without an energy buffer, implying nodes need to consume harvested energy immediately respecting the peak-power constraint. Assuming perfect causal knowledge of energy harvesting process both in encoder and decoder sides, the capacity region is derived.

Another network scale analysis is given in [18]. Under ALOHA and CSMA medium access protocols, ambient energy scavenging ad hoc wireless nodes are examined to derive the information theoretic capacity. Assuming Bernoulli distributed arrivals for energy harvests and equal transmission probabilities for each node, capacity expressions are obtained for both infinite and finite battery cases.

In general, it could be concluded that capacity of the communication schemes drastically depends on the harvesting profile, which is primarily a consequence of the type of harvester. As stated in the studies reviewed in this section, resources shall be allocated in an effective way to fully take the advantage of harvesting infrastructures and get closes to the boundaries of the achievable rate region. In the following section, efforts focusing on this area will be examined.

2.2 Resource Allocation Problems

Resource allocation problems considered within this section generally undertake different tasks, i.e., maximization of throughput, a utility function or minimization of mean delay, completion time, energy consumption etc., by manipulating the assignment of resources like energy or data in the queue. However, all of the objectives require energy efficiency as rule of thumb.

Among these allocation problems, the first study to be classified as power management for energy harvesting networks has come out in [2]. In [2], maximization of average duty-cycle of sensor nodes has been performed by fully utilizing the solar energy considering the inefficiencies caused by storage. It has been noted that, due to the storage inefficiencies direct consumption of energy rather than charging might help efficient usage of energy, while deferring the usage might also have the same effect in case of energy shortage in future times. In

general, the problem formulation in [2] was built on this dilemma and a low complexity optimal solution, increasing the duty-cycle in high recharge rate regions and lowering otherwise, is obtained.

In [2], energy harvesting profile is assumed to follow a periodic predictable structure, which is generally the case for solar harvesters, and solution is derived based on this nature. In [3], a more generic solution scheme is obtained by relaxing this assumption. Regardless of the source of energy, a computationally efficient solution structure is proposed. Again, inspiring from [2], authors have studied a more general problem [19], which is proposed to model a larger variety of application scenarios. As a matter of fact, [19] formulates a linear programming problem to capture different constraint sets and objectives, i.e., tradeoffs between memory usage and communication, maximization of minimum duty cycle etc., and includes a generic low-complexity scheme for the solution of problem.

In this sense, [4] is the last work following the footsteps of [2]. In common, studies we considered up to this point investigate the allocation of resources within the orientation of sensor network infrastructure. In [4], a periodic random field estimation application is considered and nodes are thought to sense the environment in a repetitive way followed by delivery of the packets to a central sink. For this setting, throughput and mean delay optimal policies are derived for both cases: processing costs ignored and processing costs considered.

It should be noted that, in many cases sensor nodes operate within a low-SNR region, which implies a linear transmission rate-power relationship. Studies in [2, 3, 19] restrict attention to such cases in an online manner and bases the problem formulations on some other communication tradeoffs. However, investigation of the problem from a general perspective requires a more generic consideration. Although this poses complex problem structures suffering from tractability issues, offline formulations help to forge ahead. In the rest, offline scheduling problems will be reviewed.

The basic offline scheduling problem of energy-efficient packet transmission [20, 21, 22, 23, 24] is to assign data rates (consequently transmission durations) to a set of packets whose arrival times are known in advance, so that transmission is completed within a given time window with minimum total energy. The solution needs to strike a trade-off between energy efficiency and delay: lowering energy expenditure per bit of information calls for lowering transmission rates, which causes delay. Recently, the dual problem of minimizing transmis-

sion duration of a given amount of data has been formulated with a model where energy gets “harvested” or replenished at certain known instants [25]. The irregularity in the availability of energy introduced additional richness to the problem.

While in the former formulations transmission rate needs to be adapted to the arrival rate of information, in [25] it is adapted to the rate of generation of energy. The point-to-point problem in [25] was recast for finite energy storage [26] and considering time-varying battery size together with battery inefficiencies [27]. It has been shown that, an excessive increase in transmission power might be required to prevent energy waste [26]. Moreover, a minimum energy consumption curve must be obeyed due to the battery inefficiencies [27].

The formulation has been concurrently extended to a BC in [28] and [29], considering a static pool of data to be sent at the beginning of the schedule. Deriving the structural properties of an optimal solution, different solution techniques have been proposed to achieve the best scheme. [28] proves the optimality of a polynomial time iterative algorithm while, [29] obtains the optimal solution by proving the existence of a cut-off power level and through an iterative algorithm. Additionally, the same BC problem was investigated under a limited battery constraint [30] and without static data pool assumption [6].

Next, in [7] the offline formulation was extended into a fading channel scenario considering battery size limitations. Based on the Lagrangian solution, a novel low-complexity algorithm, directional water-filling, was proposed. In addition, several sub-optimal policies are developed based on optimal solution structure and this study was followed by [31], considering fading Gaussian broadcast channel extension. Emphasizing the importance of channel state information in resource allocation problems, [32] discusses challenges regarding training optimization. Conclusion of the work in [32] states that, period and transmission power of the training sequence critically matters especially for large sized transmission blocks.

Recently, the problem is reformulated for cooperative communication systems. In [33], a two-hop transmission system, formed by source, relay and destination nodes with energy harvesting capabilities, is considered. Source and relay nodes get replenished in a synchronized fashion and finite-horizon throughput maximization problem is solved for both half-duplex and full-duplex relay cases. Next, [34] discussed the same problem for different energy arrival profiles in source and relay, which was followed by the orthogonal Gaussian relay channel study in [35].

Finally, [36] and [37] handle an offline resource allocation problem on an energy harvesting downlink. Respecting proportional fairness among users and manipulating the time slots, transmission power or rate allocation up to the channel state differences, [36] and [37] aim to maximize throughput within a frame. As a first step to the solution, [36] discusses structural characteristics of an optimal scheme and proposes a block coordinate descent based algorithm achieving partial optima of the problem. Next, analysis are further developed in [37] by investigating the power and time related structural properties under periodic harvesting profile and presenting two sub-optimal heuristics with low computational complexity.

As in many formulations summarized in this section, the scope of this thesis includes two offline scheduling problems. Additionally, the second avenue of the work is based on practicality concerns. The following section reviews the research in this context.

2.3 Implementation Oriented Studies

Design of an energy scavenging communication node is a comprehensive process, including the selection and integration of sub-units. As an example, type of the battery and source of the harvester, which have crucial affects on the design performance, should be analysed thoroughly. Ranging from solar to piezoelectric, several ambient harvesting techniques are available. Which harvesting type fits best into to the design depends on the system requirements and application type. Additionally, as stated in the previous section, resource management strategy shall be based on these design parameters. In a similar fashion, physical architecture could also be structured by the allocation technique.

As the overall system performance drastically depends on energy usage, sensor networks have come out as the most promising application area and implementation efforts have been focused on rechargeable sensor node development so far. One of the most outstanding example designs, namely *heliomote*, was introduced in [5]. Basically, combining *Mica2* sensor node, NiMH battery and a solar panel with dimensions 3.75 inches x 2.5 inches, one of the earliest sensor nodes with ambient energy scavenging capabilities has been developed in [5]. Fig. 2.1 shows a picture of the prototype.

Input requirements of resource management schemes have also been taken into account and some additional circuitry, such as energy monitoring component, was integrated into the de-



Figure 2.1: The heliomote prototype node [5].

sign. In [2], authors have gone one step further by implementing the proposed power management schemes on Heliomote prototype and verifying the analytical results.

In addition to the designs based on commercial off-the-shelf sensor nodes as in [5], some fully integrated architectures like *Everlast*, including sensor, micro-controller, radio etc., are also available [38]. Everlast nodes are formed by the combination of a supercapacitor, photovoltaic harvester, low supply current MCU and a low power transceiver. Similar to [38], authors in [39] discuss a comprehensive design, *ENS*. Harvesting solar energy for indoor sensor network applications, ENS prototype aims maximum energy efficiency by complete utilization of power management schemes.

Other than the implementations reviewed here, additional prototype designs with different types of harvesters exist [40, 41, 42, 43, 44, 45]. In addition to these prototypes, few commercial products have already edged into the market [46]. Based on such progressively increasing green and energy efficient implementations, it may be concluded that energy harvesting communication systems will become widespread in the near future. To this end, the gap between resource management and implementation oriented studies must be filled. In the second part of the thesis, this issue will be addressed.

CHAPTER 3

OPTIMAL OFFLINE ALGORITHMS

The analysis of optimal scheduling in this chapter will play an important role in gaining insights into the behaviour of a smart transmission scheme. In particular, scheduling problems are to be considered in an offline manner, all the events are assumed to be known in advance. Although this kind of prior information of data and energy arrivals may not be possible in all practical settings, the analysis of the offline optimal solution can shed light on the nature of a good power/rate policy and boundaries on the best performance. Moreover, in some certain scenarios, event sequence could be known or might be predicted beforehand. As an example, consider a sensor network application, where nodes are supplied by solar energy harvesters and deployed to monitor the environment periodically. In this scenario, packet generation and energy harvesting processes could mostly be known and the offline assumption might be a good approximation.

Besides offline problems, online formulations have also appeared in the literature. For example, [47, 48] develop online scheduling policies for multihop networks on finite-horizon and infinite horizon problem formulations, respectively. Online formulations do not lend themselves to simple structure, which is another aspect that makes the offline approach attractive.

Moreover, bounds on the performance gain of an online algorithm could be obtained through offline analysis and performance comparison of suboptimal schemes could be practicable. As none of the online transmission schemes can achieve the performance of an optimal offline policy, offline solutions provide benchmarks on the best performance that can be achieved. Furthermore, in some circumstances, optimal online solution might be too complicated to derive. In this case, the upper bound obtained through offline analysis may help understanding how well a suboptimal policy behave.

The main goal of this section is to build mathematical problem formulations covering the fundamentals of a communication system as much as possible, so that basic characteristics of a novel scheme could be understood through solution of the problems. Due to the analytical tractability issues, problem formulations need to avoid a complex structure while, it should include characterization details as much as possible.

Two different offline problem formulations will be considered within the chapter. Specifically, optimal scheduling scheme of an energy harvesting transmitter under two-user broadcast and single user fading channels are to be investigated. Let us begin with the broadcast problem in the following section.

3.1 Offline Broadcast Channel Problem

Consider a communication system formed by one transmitter and two receivers, where sender is powered by an ambient energy harvester and broadcast information bits to each user accordingly. An example illustration is depicted in Fig. 3.1. The transmitter aims to minimize overall transmission delay by assigning transmission power and rate pairs during transmission course. In this context, optimal scheduling structure of the transmitter under static data pool assumption was examined both in [28] and [29].

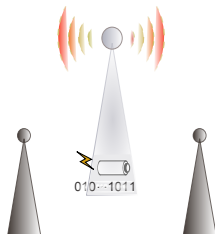


Figure 3.1: Two-user broadcast setting

Recently, the problem has been reformulated in [6] by relaxing the assumption that data is ready at the beginning of the schedule. The sender (transmitter) gets replenished with arbitrary amounts of energy as well as data packets of arbitrary length destined to each user at arbitrary points in time. The rates at which information is transmitted to each user, given a total instantaneous power, are assumed to be selected from an achievable rate region that obeys a certain structure satisfied by the additive white Gaussian noise (AWGN) BC. Studies in this section, extending the work in [6], show the structural properties of an optimal power

and rate allocation scheme for the problem.

The choices of power level and the rates to individual receivers across time is called a *schedule*. An optimal scheduling policy is defined to be one that transmits all the bits that have arrived within a certain time window, W , in the minimum possible amount of time $T^{\text{opt}} \geq W$. The policy is allowed to use as many energy harvests as it needs, provided it respects causality (no energy is used or data is transmitted before it becomes available).

This section essentially bridges the work that considered offline scheduling of *data* that becomes available at arbitrary points in time [21] on a BC and work that considered chunks of *energy* becoming available at arbitrary points in time [28] on a BC. It can also be viewed as the extension to the BC of the second problem considered in [25]. In general, main contribution in this section is the establishment of structural properties of the transmission time minimizing scheduling policy in the energy harvesting BC with packet arrivals. In addition, two different solution techniques, which are shown to be optimal in [6], will briefly be summarized to make the work solid. It is shown in section 3.2.1 that in an optimal policy, transmit power used is constant within each epoch, and may only rise from one epoch to the next, so that once it starts, the transmitter never lowers its power until it finally goes silent. On the other hand, the transmitter should increase its power only under certain conditions. These conditions, along with other structural properties of power and rate are established in section 3.1.2. We start by making the problem statement precise in the next subsection.

3.1.1 System Model

We consider a BC with one transmitter and two receivers. Arbitrary amounts of energy, $\{E_i < \infty, i = 1, 2, \dots\}$, and data destined to each user $\{B_i^{(1)}, B_i^{(2)} < \infty, i = 1, 2, \dots\}$ are obtained by the transmitter at times t_i . An example sequence of energy and data arrivals is depicted in Fig. 3.2. $E(t)$ denotes the total energy that has been *harvested* in $[0, t)$ (independent of how much of it has been consumed). Similarly, $B^{(1)}(t)$ and $B^{(2)}(t)$ stand for the total number of data destined to the first and second user, respectively, that became available to the sender within $[0, t)$. The interval between any two consecutive events (regardless of energy or data arrival) is called an inter-arrival *epoch*. Correspondingly, length of the epoch i is $\xi_i = t_i - t_{i-1}$.

Arrival times and amounts of energy and bits in the time window $t \in [0, W)$ are known by

the sender at $t = 0$. We also assumed that harvested energy and data are available for use instantaneously as they arrive. Observe that, this assumption could model a realistic battery that gets recharged at a certain rate such that the system has access to the battery only when the battery voltage exceeds a certain threshold, which indicates that it has stored a critical amount of energy. Additionally, it is assumed that transmission rate and power can be changed as soon as the decision is made. However, codeword block lengths are to be chosen in a way that each codeword is transmitted completely within an epoch (note that the beginning and the end of each epoch are known before the transmission begins), so that there is no arrival event during a codeword.

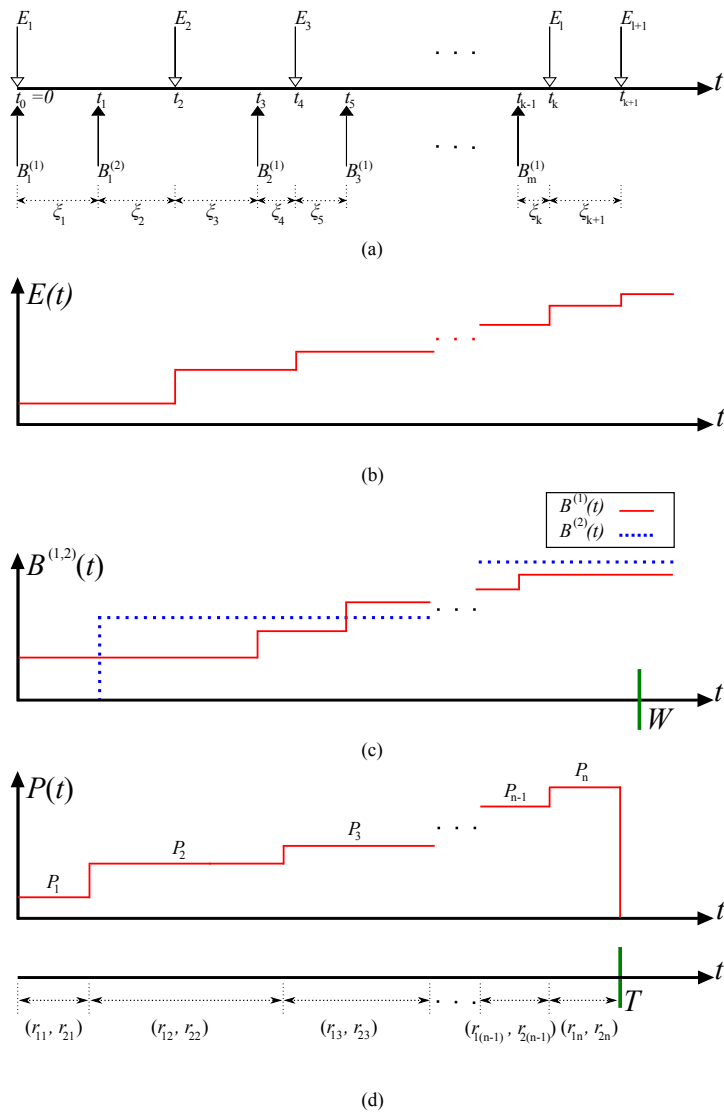


Figure 3.2: Example for (a) a sequence of energy and data arrivals, (b)-(c) the corresponding $E(t), B(t)$, (d) the schedule $P(t)$ and $\{r_{1i}, r_{2i}\}$.

The ultimate goal is to minimize the overall transmission time for packets arriving by a certain time $W < \infty$. Without loss of generality we set $B^{(i)}(t) = B^{(i)}(W)$ for $t > W$, $i = 1, 2$. To this end, we are interested in finding a schedule, composed of a sequence of power and rate allocations, completing the transmission within the minimum possible amount time. The search on attaining an optimal allocation is limited within the set of feasible allocations, sending $B^{(1)}(W) < \infty$ bits to the 1st and $B^{(2)}(W) < \infty$ to the 2nd user without violating causality (at any time, using available resources by that time). Furthermore, the achievable rate regions will be implicitly assumed to correspond to a certain constant tolerable error probability respecting which it is possible to transmit a finite number of bits with a finite amount of energy per bit.

The structure of the achievable rate region will be based on the two-user AWGN BC. The capacity region of a two-user discrete time AWGN BC with average power constraint P , noise variance σ^2 , where the 1st user's channel gain ($s_1 > 0$) is larger than the 2nd user's ($s_2 > 0$), consists of rate pairs (r_1, r_2) satisfying:¹

$$r_1 \leq \frac{1}{2} \log_2 \left(1 + \frac{s_1 \alpha P}{\sigma^2} \right) \quad \text{bits/channel use} \quad (3.1)$$

$$r_2 \leq \frac{1}{2} \log_2 \left(1 + \frac{s_2 (1 - \alpha) P}{s_2 \alpha P + \sigma^2} \right) \quad \text{bits/channel use.} \quad (3.2)$$

Here α , ($0 \leq \alpha \leq 1$), denotes the fraction of P used for the 1st user. Since $s_1 > s_2$, the 1st user will be referred as the “stronger user”, and the 2nd as the “weaker user”. Using capacity achieving codes, the rate pair (r_1, r_2) can be selected from the boundary of the rate region, where inequalities in (3.1) and (3.2) become equalities. Combining these equalities, power can be expressed in terms of the user rates, $P = g(r_1, r_2)$. Moreover, each user's rate can be expressed as a function of P and the other user's rate, such as $r_1 = h_1(P, r_2)$, $r_2 = h_2(P, r_1)$. The rate functions h_1 and h_2 defined on $\mathfrak{R}^+ \times \mathfrak{R}^+$ will be assumed to satisfy the following properties:

1. Nonnegativity: $h_1(P, r) \geq 0, h_2(P, r) \geq 0$.
2. Monotonicity: $h_1(P, r), h_2(P, r)$ are both monotone decreasing in r , and monotone increasing in P .
3. Concavity: $h_1(P, r), h_2(P, r)$ are concave in P and r : $\frac{\partial^2 h_i(P, r)}{\partial P^2} \leq 0, \frac{\partial^2 h_i(P, r)}{\partial r^2} \leq 0$, for $i \in 1, 2$.

¹ We follow the convention used in [25] for the problem definition. Therefore, rate expressions are given in bits per transmission unit.

4. $\frac{\partial^2 h_1(P,r)}{\partial r \partial P} \geq 0, \frac{\partial^2 h_1(P,r)}{\partial P \partial r} \leq 0.$
5. $\frac{\partial^2 h_2(P,r)}{\partial r \partial P} = 0, \frac{\partial^2 h_2(P,r)}{\partial P \partial r} = 0.$

The results in the rest of the section will be valid for any rate function satisfying (1)-(5), which are also satisfied by the AWGN BC [28].

It is established in the following lemma that one can limit attention to schedules that do not change their power and rate allocations within epochs.

Lemma 3.1.1 *In an optimal schedule, the power and rate pair remain constant within each epoch, except for the epoch during which the schedule ends.*

Proof. During an epoch, there are no energy or data arrivals and the claim is identical with the one stated and proved in Lemma 2 of [28]. The power will drop to zero when the schedule ends, which is in general within (and not necessarily at the end of) the last epoch used by the schedule. ■

Accordingly, let P_i be the total transmit power and r_{ji} be the rate assigned to the j^{th} user during epoch i . We are now ready to state the problem in terms of power and rate allocations to epochs, more precisely, an assignment of total power and the stronger user's rate to each epoch (the weaker user's rate is then determined by $r_{2i} = h_2(P_i, r_{1i})$). A final technical assumption will be useful in stating the problem: we shall assume that there is some $k^{\text{up}} < \infty$ such that there is at least one feasible schedule that ends within the first k^{up} epochs. In other words, k^{up} is an upper bound for both the number of epochs and the number of harvests to be considered (please see Fig. 3.2(a)). If $k^* + 1$ denotes the number of epochs used by an optimal schedule, then $k^* + 1 \leq k^{\text{up}}$.

Problem 1 Transmission Time Minimization of Data Arriving at Arbitrary Points on an Energy Harvesting BC:

Minimize: $T = T(\{P_i, r_{1i}\}_{1 \leq i \leq k^*})$

subject to: $P_i \geq 0, 0 \leq r_{1i} \leq h_1(P_i, 0), r_{2i} = h_2(P_i, r_{1i})$

$$\sum_{i=1}^k P_i \xi_i \leq E(t_k)$$

$$\sum_{i=1}^{k^*} P_i \xi_i + P_{(k^*+1)}(T - \sum_{i=1}^{k^*} \xi_i) \leq E(T) \quad (3.3)$$

$$\sum_{i=1}^k r_{1i} \xi_i \leq B^{(1)}(t_k), \quad \sum_{i=1}^k r_{2i} \xi_i \leq B^{(2)}(t_k) \quad (3.4)$$

for $k = 1, 2, \dots, k^* = \max\{i : \sum_{j=1}^i \xi_j < T\}$

$$\sum_{i=1}^{k^*} r_{1i} \xi_i + r_{1(k^*+1)}(T - \sum_{i=1}^{k^*} \xi_i) = B^{(1)}(T)$$

$$\sum_{i=1}^{k^*} r_{2i} \xi_i + r_{2(k^*+1)}(T - \sum_{i=1}^{k^*} \xi_i) = B^{(2)}(T) \quad (3.5)$$

We will refer to (3.3) and (3.4) as energy and data causality constraints, respectively, as these ensure no energy is consumed and no bit is transmitted before becoming available. In addition, when the k^{th} inequality in (3.3) holds with equality, we shall say that k^{th} energy constraint is active. Similarly, equality case in (3.4) will be referred as a data constraint being active. Finally, the feasibility constraint (3.5), ensures all the data bits destined to each user are transmitted.

In the next subsection, we investigate structural properties that any optimal schedule has to satisfy.

3.1.2 Structure of an Optimal Policy

Lemma 3.1.1 recorded that in an optimal schedule power can only change upon a data arrival or energy harvest. The next result states that when power changes, it can only increase. The key to the proof is that more “bits per joule” can be sent by evenly distributing energy across a time interval (i.e., maintaining a constant power level, which is a consequence of the concavity properties of our rate functions.) If an even distribution of power requires transferring energy or bits to the latter epoch, it can always be done; hence, total transmit power never decreases

in time. But, power may increase in time, because even distribution of power may result in unmet causality constraints. We state these results in Lemma 3.1.2.

Lemma 3.1.2 *Consider an optimal schedule that ends during epoch $k^* + 1$. Power is non-decreasing with epoch index, i.e, $P_i \leq P_{i+1}$ for $i = 1, 2, \dots, k^*$.*

Proof. See Appendix A

As stated in Lemma 3.1.2 power cannot decrease, yet may rise in time like a staircase function formed bands of constant power that last for several epochs (see Fig. 3.2(d)). In the next lemma we note a necessary condition for such a rise to occur in an optimal policy.

Lemma 3.1.3 *In an optimal policy, power can only rise at t_i (end of epoch i) if at least one of the conditions below holds:*

1. Energy constraint is active at point t_i . (i.e., the i th energy constraint is active)
2. The data constraints for both users are active at point t_i . (i.e., the set of constraints in (3.4))
3. The weaker user's data constraint is active and data arrival to the weaker user occurs at time t_i .

Proof. See Appendix B

The next set of results illustrate the structure of *rate allocation* in conjunction with the power allocation in an optimal policy.

Corollary 1 *In an optimal policy,*

1. *If power increases upon a data arrival for the weaker user, all available data destined to the weaker user have been transmitted by this point in time.*
2. *If power rises upon a data arrival for the stronger user, all available bits have been sent by this event.*

3. *If power increases upon an energy harvest, all energy available at the beginning of the former constant power band has been consumed by this energy harvest.*

Proof.

1. Suppose that power increases upon a bit arrival for the weaker user occurring at t_i . As there is no energy constraint at t_i , bringing power levels closer does not contradict with the energy causality in this case. This implies that conditions (b) or (c) stated in Lemma 3.1.3 must hold. However, we know that there is a data arrival for the weaker user at t_i , so if (b) were true, then (c) would be true as well. Therefore, condition (c) holds in either case.
2. Suppose that power increases upon a bit arrival for the first user. With similar reasoning to part-1, condition (a) of Lemma 3.1.3 cannot hold. As there is also no data arrival for the weaker user, condition (b) must be satisfied.
3. As there is no data arrival at the time when power increases, the only possibility that power increases upon an energy harvest is condition (a) of Lemma 3.1.3. ■

Aside from the properties listed here, one can easily show that, an optimal policy should consume all the harvested energy by the end of transmission. Additionally, some further structural properties could be obtained under special conditions stated as in [6]. Solution of Pr. 1 have been discussed in [6] exhaustively. To provide integrity, we summarize the main points of the solution in the following subsection.

3.1.3 Solution of Offline Broadcast Problem

Formulation of the Problem 1 doesn't obey the structure of a classical convex optimization program, implying convex optimization techniques cannot be applied directly to obtain an optimal solution. Based on the structural properties listed in the former subsection, a novel solution technique, namely *DuOpt*, has been proposed in [6]. *DuOpt* algorithm has been developed following similar lines with the solution technique *FlowRight*, which was shown to be the optimal solution of Pr. 1 under static data pool assumption. Starting with a certain structured feasible schedule, *DuOpt* sequentially updates rates assignments to each epoch.

In each step, the algorithm revises each user's rate on a single epoch pair. Optimizing the assignment over sequential pairs, the method aims to converge to the global optimal (For a detailed discussion on DuOpt see [6]).

Another solution technique presented in [6] is a convex optimization method. As mentioned before, convex optimization techniques cannot be applied directly to the problem as it has not been shown to be convex. However, it was applied through an equivalent convex problem in [6]. By iteratively solving the equivalent problem by *SUMT* method, original solution is shown to be attainable. In latter sections of this thesis, we will follow a similar path to obtain the solution of a different optimization problem and details of the method will be discussed thoroughly.

In [6], DuOpt and SUMT methods are compared by means of main points. Although optimality of DuOpt has not been proven in general case, it is shown to return the optimal solution in a special but quite general case. In addition, DuOpt is observed to return the same results with SUMT in all numerical trials. It is noted that, DuOpt is a significantly faster method than SUMT and terminates within an approximately two orders of shorter length duration.

Our analysis continues with a different problem setting in the following section.

3.2 Single User Offline Fading Channel Problem

In chapter 2, a few offline fading channel scheduling problems were presented, including the solution of the transmission completion time minimization problem with a static data pool and known harvest times and channel states [7].

In this section, we extend the formulation of [7] by relaxing static data pool assumption and contribute to the previous work by developing an offline solution for the time minimizing packet scheduling problem under fading conditions. The solution needs to adjust its transmission power and rate over the course of transmission with respect to packet arrivals, as well as channel state and energy harvests. This will sometimes correspond to lowering rate (therefore the energy per bit), to work energy efficiently and prevent premature data queue idleness; and at other times, increasing the rate to take advantage of a good channel state, especially when energy is abundant.

After making the problem statement precise, the uniqueness of its solution is shown through equivalence to a related energy minimization problem. The solution is first obtained for the equivalent convex problem by unconstrained sequential minimization technique (SUMT) and the optimal allocation of the completion time minimization problem is shown to be achievable through iterative runs of SUMT. We begin with the problem statement in the next section.

3.2.1 System Model

Consider point-to-point communication over a fading channel, where transmission is supplied by the harvested energy, arriving at arbitrary instants. Accordingly, in discrete-time, the received signal is $y = \sqrt{h}x + n$, where x and \sqrt{h} are the input symbol and channel gain, and n is zero-mean unit variance Gaussian noise. Following the offline formulation in [7], the transmitter is assumed to have knowledge of the energy harvests as well as channel states before transmission starts. In contrast to [7], data packets are allowed to arrive at arbitrary (known) times during the course of transmission. The harvested energy is stored in an (ideal) battery and immediately becomes available for use by the transmitter. Data packets are stored in a data buffer (of infinite capacity.) An example sequence of energy and packet arrivals, as well as channel gain changes is illustrated in Fig. 3.3. Starting from time $t_1 = 0$, the amounts of energy and data have become available by time t are denoted by $E(t)$ and $B(t)$, respectively. Any arrival of energy or data or a change in the channel state is called an *event*. The duration between any two consequent events is called an epoch. The length of i^{th} epoch is $\xi_i = t_{i+1} - t_i$. Given an average power constraint p_i and channel gain level $\sqrt{h_i}$ during the i^{th} epoch, we assume rate level of $r_i = \frac{1}{2} \log_2(1 + h_i p_i)$ is achievable for a certain tolerable error probability. Equivalently the power level used to transmit a codeword at rate r_i is given by: $g(r_i) = \frac{2^{2r_i} - 1}{h_i}$.

Packets arriving in a certain time window of size $W < \infty$ are considered. The problem is to find an allocation of power and rate across time that minimizes the total duration of transmission for all of these packets. An optimal policy should respect causality constraints (at any time, only the resources available up to that point can be used). It immediately follows from the concavity of the rate function that rate (and power) should not change within an epoch. So, the search for an optimal schedule can be limited to schedules that keep a constant power level and rate within each epoch. Hence, the optimization problem can be written in

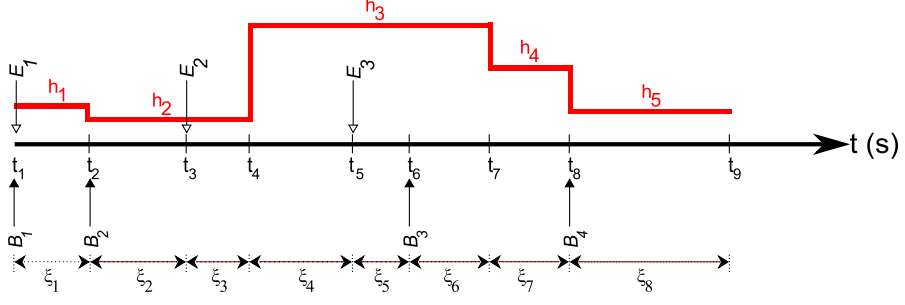


Figure 3.3: An example sequence of events: $t_i, i \geq 1$ are event times (energy harvests marked as E_i , channel state changes, h_i , or data arrivals B_i). The ξ_i denote inter-event epoch durations.

terms of rates assigned to epochs. Note that in the problem formulation below, the solution space is further limited (w.l.o.g.) to schedules spanning no more than some k^{up} epochs. The value of k^{up} can be set as the number of epochs used by any arbitrary feasible schedule.

Problem 2 Transmission Time Minimization of Packets on an Energy Harvesting Fading Channel:

$$\text{Minimize: } T = T(\{r_i\}_{1 \leq i \leq k^{\text{up}}})$$

$$\text{subject to: } r_i \geq 0$$

$$\sum_{i=1}^k g(r_i) \xi_i \leq E(t_k), \quad (3.6)$$

$$\sum_{i=1}^k r_i \xi_i \leq B(t_k) \quad (3.7)$$

$$\sum_{i=1}^{k^*} r_i \xi_i + r_{k^*+1} (T - \sum_{i=1}^{k^*} \xi_i) = B(T) \quad (3.8)$$

$$\text{for } k = 1, 2, \dots, k^* = \max\{i : \sum_{j=1}^i \xi_j \leq T\}$$

In Pr. 2, k^* denotes the last epoch used in an optimal schedule. (3.6) and (3.7) state the (energy and data) causality constraints, while (3.8) ensures transmission completion of all data. Following [6], the equivalence of Pr. 2 to a convex problem, namely Problem 3, will be exhibited.

3.2.2 An Equivalent Problem

Problem 3 aims to find a schedule which minimizes total energy consumption to transmit a given sequence of packets within a given deadline constraint T , using the energy harvested during this time.

Problem 3 Energy Consumption Minimization of Packets on an Energy Harvesting Fading Channel:

$$\begin{aligned} \text{Minimize: } E^c(T) &= \sum_{i=1}^{k^*} g(r_i)\xi_i + g(r_{k^*+1})(T - \sum_{i=1}^{k^*} \xi_i) \\ \text{subject to: } r_i &\geq 0 \end{aligned} \quad (3.9)$$

$$\sum_{i=1}^k g(r_i)\xi_i \leq E(t_k) \quad (3.10)$$

$$\sum_{i=1}^k r_i\xi_i \leq B(t_k) \quad (3.11)$$

$$\sum_{i=1}^{k^*} r_i\xi_i + r_{k^*+1}(T - \sum_{i=1}^{k^*} \xi_i) = B(T) \quad (3.12)$$

$$\text{for } k = 1, 2, \dots, k^* = \max\{i : \sum_{j=1}^i \xi_j \leq T\}$$

Lemma 3.2.1 *Problem 3 is a convex optimization problem.*

Proof. Firstly, note that $g(r_i)$ is a strictly convex, monotonically increasing function. Furthermore, the constraint set of the problem is defined by non-negative weighted sums of either $g(r_i)$'s and r_i 's, each constraint being either convex or linear, respectively. It easily follows (please see Appendix C for details) that the set of feasible allocations form a convex region. Finally, as the objective function of the minimization problem is also a non-negative weighted sum of increasing convex functions, we conclude that Pr. 3 is convex [49].

Lemma 3.2.2 *Suppose T is the minimum completion time (obtained by solving Pr. 2) for the sequence of packets arriving by time W , $0 < W \leq T$. Then, for this sequence of events, any solution of Pr. 3 with deadline constraint specified as T provides a solution to Pr. 2.*

Proof. Let schedules S^1 and S^2 be optimal solutions of Pr. 2, and Pr. 3, defined with the deadline T , respectively. The energy consumption of both schedules must be the same since

the opposite claim would contradict the optimality of the schedules: S^2 has used no more energy by T than S^1 , by definition. Suppose it used less energy, than this means that S^1 has used some extra energy to transmit the same packets as S^2 . But then, it could use this extra energy in the last epoch to reduce the completion time by a nonzero amount, which would contradict optimality. Hence, we have 2 schedules completing the transmission of the same amount of data at the same time by consuming same amount of energy. Thus, S^1 and S^2 are both solutions to problems 2 and 3. ■

Corollary 2 *Solution of Pr. 2 is unique.*

Proof. As any solution of Pr. 2 provides a solution to Pr. 3, in order for Pr. 3 to have a unique solution (which is true by convexity) Pr. 2 must have a unique solution. ■

3.2.3 Solution of Problem 3

The *sequential unconstrained minimization technique (SUMT)* is a convenient method [50, 51] for iteratively converging to the optimal of a constrained problem by solving a sequence of unconstrained optimization problems. The unconstrained problems are formed by adding to the objective of the original problem penalty terms corresponding to constraint violations. Correspondingly in our case, Pr. 4 is obtained as follows:

Problem 4 Unconstrained Minimization Problem:

$$\text{Minimize: } F(\mathbf{r}) = \left(\sum_{i=1}^{k^*} g(r_i)\xi_i + g(r_{k^*+1})(T - \sum_{i=1}^{k^*} \xi_i) \right) + \mu P(\mathbf{r}),$$

$$\text{where, } P(\mathbf{r}) = \sum_{i=1}^{k^*+1} (\max(0, -r_i))^2 \quad (3.13)$$

$$+ \sum_{k=1}^{k^*+1} \left(\max(0, \sum_{i=1}^k g(r_i)\xi_i - E(t_k)) \right)^2 \quad (3.14)$$

$$+ \sum_{k=1}^{k^*+1} \left(\max(0, \sum_{i=1}^k r_i\xi_i - B(t_k)) \right)^2 \quad (3.15)$$

$$+ \left(\sum_{k=1}^{k^*} r_k\xi_k + r_{(k^*+1)}(T - \sum_{i=1}^{k^*} \xi_i) - B(T) \right)^2 \quad (3.16)$$

Due to constraints (3.9),(3.11) and (3.12), penalty terms (3.13), (3.14), (3.15) and (3.16) have been added to the objective function. Starting from a point in the exterior of the feasible region for an initial value of the penalty coefficient $\mu = \mu_0$, the next point is reached by solving the corresponding unconstrained minimization problem. At each SUMT iteration, initial point is moved to the previously computed result. By iterating the penalty coefficient such that after iteration n , $\mu^n = \eta\mu^{n-1}$ for some growth parameter $\eta \geq 1$, a sequence of unconstrained problems with monotonically increasing values of the penalty coefficient is solved. Intuitively, this drives the points toward the feasible region. It is proved in [50] that in the case of a convex objective and penalty terms as defined above, the algorithm converges to the optimum of the original constrained problem as μ goes to infinity. In practice, the iterations are stopped when an arbitrary stopping criterion $1/\mu \leq \epsilon_S$ is satisfied.

In our problem, SUMT is initialized with an infeasible allocation (i.e., at a point in the exterior of the constraint region), specifically, transmitting all data at constant rate within the given deadline T , disregarding causality constraints. To ensure fast convergence (see [50, 51]) μ is initialized such that the values of the objective and penalty terms are commensurate, and the penalty terms corresponding to each constraint are scaled such that no constraint dominates. Algorithm 1 outlines the method from a general perspective.

Algorithm 1 SUMT Algorithm

- 1: $r_i \leftarrow \frac{B(T)}{T}, \mu \leftarrow \text{initial value}$
 - 2: **repeat**
 - 3: $\mathbf{r} \leftarrow \text{InnerMethod}(\mathbf{r})$
 - 4: $\mu \leftarrow \eta\mu$
 - 5: **until** $\mu \geq \mu_{max}$
-

At each iteration of SUMT, the corresponding unconstrained problem is solved by *Newton's method*. It is quite standard to apply Newton's method in the inner iterations of SUMT. After the l^{th} Newton step in an inner iteration, rate allocation vector is updated as: $\mathbf{r}^{l+1} = \mathbf{r}^l - [[\nabla^2 F(\mathbf{r}^l)]^{-1} \nabla F(\mathbf{r}^l)]$. The *Newton decrement*, $\lambda(\mathbf{r}^l) = \left(\nabla F(\mathbf{r}^l)^T [\mathbf{H}F(\mathbf{r}^l)]^{-1} \nabla F(\mathbf{r}^l) \right)^{\frac{1}{2}}$, becoming smaller than a predefined accuracy parameter ϵ_N is the stopping criterion for each inner iteration. By reducing ϵ_N , the inner optimizations can be made arbitrarily accurate [49]. The method is summarized in Algorithm 2.

The convergence rate of these iterations will be discussed in the following sections.

Algorithm 2 Newton's Method

```
1: repeat
2:    $F_{Previous} \leftarrow F(\mathbf{r})$ 
3:    $\Delta \mathbf{r} = -[\mathbf{H}F(\mathbf{r})]^{-1} \nabla F(\mathbf{r})$ 
4:    $\lambda(\mathbf{r}) = \left( \nabla F(\mathbf{r})^T [\mathbf{H}F(\mathbf{r})]^{-1} \nabla F(\mathbf{r}) \right)^{\frac{1}{2}}$ 
5:    $\mathbf{r} \leftarrow \mathbf{r} + \Delta \mathbf{r}$ 
6: until  $\lambda(\mathbf{r}) \leq \epsilon_N$ 
```

3.2.4 Solution of Problem 2

From Lemma 3.2.2 , using the optimal value of completion time, T^{opt} , as a parameter in Pr.2 would give us an optimal schedule for Pr.1. Of course, T^{opt} is not known before solving Pr.1. The method we will use is to iteratively approach T^{opt} by solving Pr. 2 for different values of

Algorithm 3 Time Minimization with SUMT Algorithm

```
1:  $N \leftarrow \underset{k \in \{1, 2, \dots, k^{up}\}}{\text{argmin}} (B(t_{k^{up}}) = B(t_k))$ 
2: repeat
3:    $N \leftarrow N + 1$ 
4:    $E_{min} \leftarrow \text{SUMT\_Algorithm}(t_N)$ 
5: until  $E_{min} \leq E(t_N)$ 
6:  $T^{min} \leftarrow t_{N-1}$  ,  $T^{max} \leftarrow t_N$ 
7: repeat
8:    $T \leftarrow (T^{min} + T^{max})/2$ 
9:    $E_{min} \leftarrow \text{SUMT\_Algorithm}(T)$ 
10:  if  $E_{min} < E(T)$  then
11:     $T^{max} \leftarrow T$ 
12:  else
13:     $T^{min} \leftarrow T$ 
14:  end if
15: until  $T^{max} - T^{min} \leq \epsilon_b$ 
16:  $T_{min} \leftarrow T$ 
```

T and checking the resulting amount of energy consumption. The bisection method will be used to monotonically narrow down the interval in which the optimal completion time T^{opt} of Pr. 2 must lie in. Since $E(T)$ is a monotonically decreasing and continuous function of T [6], any feasible value of T provides an upper bound on T^{opt} . In search of upper and lower bounds, T is initialized as the end of last data arrival epoch, and SUMT is run as detailed in

Section 3.2.3. If the resulting optimal energy that SUMT returns is too high, it means that transmission cannot be completed within this deadline, hence the current value of T provides a lower bound. T is then extended by the next epoch length. This procedure is repeated until the total consumed energy returned by SUMT goes below the energy harvested by T . That value of T provides an upper bound. The next deadline is chosen as the average of the upper and lower bounds, and SUMT is run again. If the deadline is feasible, it becomes the new upper bound, if not, it becomes the new lower bound, and so on. The iterations are stopped when the difference between the upper and lower bounds goes below ϵ_b , which, provided that the inner optimizations of SUMT are also done with sufficient accuracy, sandwiches T^{opt} in an interval of size ϵ_b . In Algorithm 3, this process is described.

3.2.5 Computational Complexity

The computational complexity is largely imposed by the stopping criteria of Newton, SUMT and bisection iterations. To compute the overall complexity of proposed scheme, let us first consider the number of bisections. When bisection iterations begin, the difference between upper and lower bounds on completion time becomes the last epoch length of the most current schedule returned by SUMT. In each iteration this interval is halved, so at most $\lceil \log_2(\xi_{k^*+1}/\epsilon_b) \rceil$ bisections are to be performed. For each bisection, SUMT makes $\lceil \log(\frac{1}{\mu\epsilon_S})/\log(\eta) \rceil$ iterations to converge with a desired accuracy of ϵ_S [49]. The number of Newton steps to achieve an accuracy of ϵ_N in the inner Newton iterations per each iteration of SUMT is upper bounded by $\frac{F(\mathbf{r}^0)-F^*}{\gamma} + \log_2 \log_2(1/\epsilon_N)$, where γ is the minimum decrement amount of F and F^* is the value at the optimal point [49]. This bound follows from the different nature of convergence of Newton's iterations for different operating points. It has been shown in [49] that, once the operation point gets sufficiently close to the optimum, convergence rate is quadratic, while it is approximately linear until then. Finally, the computational requirements imposed by each Newton step, due to the construction and the inversion of a $2k \times 2k$ Hessian (where k is the number of epochs in the problem), is polynomial (with complexity $O(k^3)$ or as low as $O(k^2)$ with ultimately efficient implementation.)

3.2.6 Numerical Results

As an example, consider the event sequence depicted in Fig. 3.4. The final schedule returned by the proposed algorithm is also shown in the figure. The penalty parameter μ is initialized as 1, the growth parameter η is set to 2. The threshold values for Newton's method, SUMT and bisection are 10^{-8} , 10^{-10} and 10^{-3} , respectively. The algorithm repeats 34 SUMT iterations, within which at most 6 Newton's steps are repeated, for each of 12 bisection repetitions and terminates within 95 seconds in MATLAB running on a MacBook Pro rev. 8.1. When the Newton's and bisection thresholds are raised to 10^{-3} and 10^{-2} , respectively, the run time reduces to 15 seconds. It is most likely to be that optimizing the code over an efficient programming platform can reduce this time significantly. On closer examination of the final schedule, it can be observed that variations in channel state and arrival events have strong influences on the structure. When the event sequence in Fig. 3.4 is considered, rare data arrivals in addition to the high channel gain states can be noticed within the first half of the transmission course. Therefore, optimal assignment takes the advantage of good channel states and completes transmission of feasible data until $t = 6s$. By doing so, it aims to consume the minimum possible amount of energy and conserve the rest for the rest of the transmission. During the next two epochs, the same strategy is repeated and the transmission is finalized by sending the data accumulated from the last arrival event with the remaining amount of energy.

Next, another example run of SUMT is given in Fig. 3.5. In this example, the algorithm performs the same number of iterations for the threshold values given in the previous examination. Note that, optimal schedule defer transmission during the 2^{nd} epoch since the channel is in deep fade. However, it does not decrease transmit power level significantly during the last epoch, where channel gain is respectively low, since there occurs a data arrival at the beginning of the epoch. As enough amount of data is accumulated and channel gains are respectively high by the end of the third epoch, all the harvested energy is consumed. During the rest of the scheduling course, energy arrivals occur more often. Consequently, the transmitter further increases power level to the complete the transmission as soon as possible. Finally in the last epoch, the algorithm assigns the constant power level respecting energy causality to transmit the remaining bits within the minimum possible amount of time.

In this section, a method for solving the offline minimum completion time packet scheduling problem on an energy harvesting fading channel has been developed and demonstrated. The

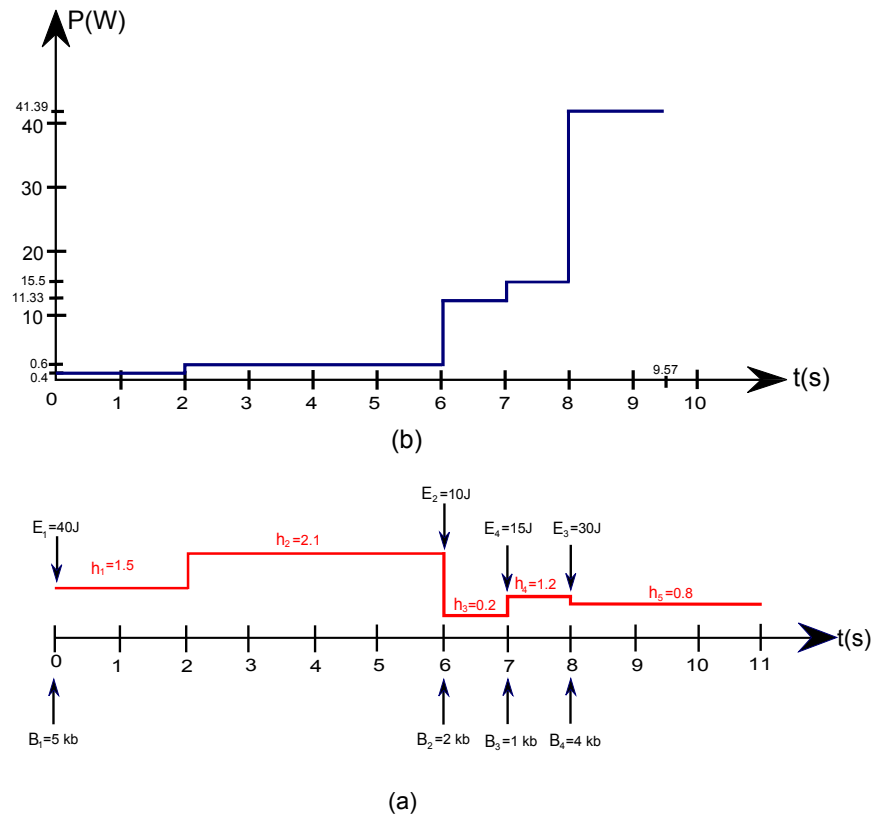


Figure 3.4: (a) An example event sequence. The squared channel gain in the i^{th} epoch is h_i , the bandwidth is $W = 1$ KHz, energy harvest amounts and arriving data are marked as E_i and B_i , respectively. (b) Final schedule returned by completion time minimization algorithm.

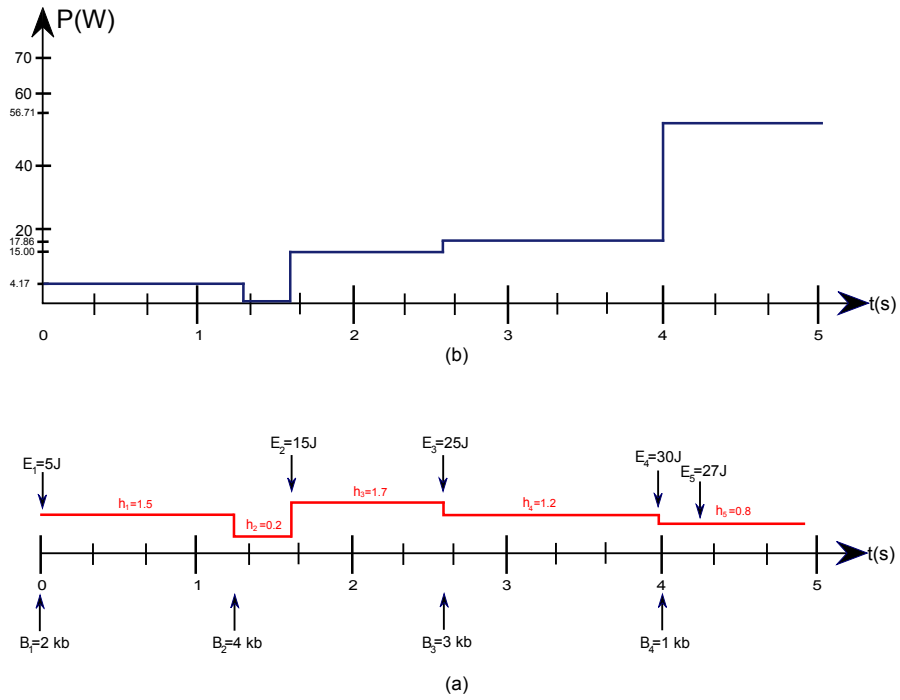


Figure 3.5: (a) An example event sequence. The squared channel gain in the i^{th} epoch is h_i , the bandwidth is $W = 1$ KHz, energy harvest amounts and arriving data are marked as E_i and B_i , respectively. (b) Final schedule returned by completion time minimization algorithm.

key to the method is exhibiting equivalence to an energy minimization problem which is a convex program. In certain realistic scenarios, the harvest profile and data arrivals may be known in advance. In that case, the offline solution would apply for a static channel. On a fading channel with an ergodic channel state process, an online algorithm such as waterfilling could run on top of the offline adaptation. When the data and/or harvest arrivals are also unknown, the offline solution here may be combined with a prediction or learning scheme or a simple look-ahead policy. With this offline formulation, we conclude theoretical approaches to the problem. In the rest, research will be oriented based on practicality and implementation concerns.

CHAPTER 4

AN IMPLEMENTABLE ALGORITHM: TriMod

Adaptive transmission, also known as adaptive coding and modulation has appeared in research papers for at least two decades, and in standards for at least a decade, as a mechanism for using wireless channels efficiently. Optimal adaptation of rate and transmit power for various objectives has been well understood. However, the implementation of such adaptive schemes has progressed relatively slowly due mostly to the practical difficulties involved in dynamically changing the operating regime of a transceiver, such as, the inefficiency incurred when transmit amplifiers are used in a wide dynamic range. However, adaptation has been more common recently, among new generation communication devices and, certainly new standards such as the newer 802.11 versions and 802.16, as well as Long Term Evaluation (LTE). Along these lines, the ideas behind theoretical studies should go from conception to maturity, and thus implementable heuristics shall be proposed.

So far, all the discussions could be thought as the steps to achieve the ultimate goal of producing more efficient, conventional and optimized final products. In this context, next move would be the consideration of practicality issues of resource management schemes. Even though offline scheduling analysis provide foreknowledge into the design of a rational implementable transmission technique, additional efforts need to be performed to accomplish the work. Specifically, as discussed in the previous sections, the scope of analytical and implementation related research should become more relevant. To this end, design process should include interactions between these two studies. Inherently, practicality and physical concerns posed by the system characteristics are readily taken into consideration by implementation oriented work. Accordingly, these constraints shall be considered in analysis, as ignoring them may cause serious performance degradation. Similarly, physical design should

be structured according to the implications of analysis. As an example, effect on the choices of physical hardware components by memory and processing requirements or development of additional circuitry to provide essential inputs of the transmission scheme might be given.

Throughout this chapter, we will focus on the design of an implementable adaptive transmission rate, code rate and modulation scheme correspondingly, and power strategy along with the implications of constraints posed by practicality and implementation issues. Specifically, each challenge will be covered explicitly. Afterwards, the proposed implementable algorithm will be introduced starting with basic intuitions of the design. Next, we will give a comprehensive performance analysis through a special communication setting and conclude the chapter with the implementation of the algorithm over GNU Radio framework and USRP hardware. In the following section, practicality issues will be discussed.

4.1 Implementability Concerns

Conventional rate adaptation protocols adjust modulation and coding rates according to channel quality, data queue and application type. Likewise, power management schemes follow a similar path. As an example, 802.11 family devices support rate adaptation based on link quality, i.e., the better the link, the higher the rate. As regards energy harvesting transmission settings, additional adaptation basis such as battery or recharge state could be required, implying design and development of additional hardware.

In a similar fashion, interactions between different transmission layers might be imposed by the adaptation algorithms. Cross-layer design of wireless communication systems has drawn considerable attention [52, 53, 54, 55] in the last decade. To accomplish a complete enhancement and optimize the overall system operation, rather than individual consideration of each layer a massive analysis of the transmission setting is shown to be worthwhile. In this context, a deeper understanding of cross-layer interactions, especially between physical layer technologies and higher layer protocols, has to be gained so that corresponding requirements on each layer could be met. However, cross-layer adaptation schemes might not be practical in some scenarios, i.e., interfering the design of an existent layer could not be possible or development and interlayer optimization processes might be too costly. In such cases, constraints posed by cross-layer adaptation shall be reconsidered.

Alongside additional hardware and middleware necessities, there are some physical constraints. In the following subsections, the most prominent limitations will be covered. Firstly, we shall consider implications of limited data rate selection.

4.1.1 Discrete Set of Data Rates

Due to the analytical tractability concerns, many of the adaptive transmission investigations assume that code rate can be continuously varied. As in the way that we have followed in the previous chapter, such analysis provide strong insight into the problem. However, this idealized assumption does not hold in modern communication systems. Ranging from *IEEE 802.11* to 3rd and 4th generation transmission protocols, rate adaptation is based on selecting one out of a finite family of coding and modulation schemes.

Many physical layer protocols support transmission on several data rates through a combination of various code rate and modulation scheme. While, lower rates are more reliable, higher rates perform better by means of delay considerations. In terms of energy efficiency, lower rates are preferable under the same target bit error rate (BER), channel quality and interference conditions. In overall, energy efficiency, delay and reliability tradeoffs hold in many transmission settings. However, as in *IEEE 802.15.4*, efficient energy usage-delay tradeoff may not be as strong or severe, in case of low-SNR region operation. Likewise, rate-reliability characteristics might be distorted due to frequency drift and bad spatial structure of the medium as stated in [53]. While defining the problem and determining solution strategies, these characterizations should be carefully addressed.

4.1.2 Power Amplifiers

Output RF power of common transmitters are arranged by a power amplifier deployed in RF front-ends. Mostly based on channel quality metrics, power adaptation schemes are performed to utilize channel conditions effectively or to compensate variations of channel state for the receiver. Commonly, it is assumed that, increasing the input power will also increase SNR at the receiver, improving received signal quality, and thus reducing error probability. However, this assumption doesn't hold in the most general form, since power amplifiers have non-linear amplification regions. While operating inside linear amplification region sig-

nal strength is improved along with the increased input power level, unforeseeable outcomes rather than the expected characteristics would be observed within the non-linear region. Thus, operation of amplification is limited within linear region. An adaptation scheme should be aware of the linear range of the power amplifier and act accordingly, otherwise serious performance degradation becomes inevitable.

Observe that, linear range of the amplifier upper bounds the maximum output transmit power level. This effect is more noticeable in orthogonal-frequency division multiplexing (OFDM) systems due to the peak to average power ratio constraint. Although not required by this limitation, achievable transmit power levels may be approximated as a finite set, just like set of achievable transmission rates. As a matter of fact, this approximation is more realistic. Thus, structuring the allocation scheme based on this limitation seems to be more reasonable. After the discussion on characteristics of adaptation variables, we next consider channel estimation issue.

4.1.3 Adaptation to Channel State

As in the traditional allocation algorithms, channel quality parameters may be used as a basis for adaptation schemes of energy harvesting communication systems. As a matter of fact, to fully enhance the operation and achieve a performance near capacity, adjustment up to the channel state changes is necessary [56]. However, gathering explicit side information of the link is a real challenge. Thus, as regards practical allocation algorithms this issue needs to be carefully addressed.

Essentially, fluctuations on channel quality, *fading*, arises due to the relative mobility of transmitter, receiver or scatterers. [54] has categorized adaptation to fading under two types: *loss-triggered* and *SNR-triggered*. While loss-triggered adaptation protocols make decisions based on consecutive delivery failures and successes, in SNR-triggered allocation schemes, signal-to-noise ratio is calculated by the receiver and the transmitter gets informed about the allocation decision via a four-way handshake.

Different loss and SNR-triggered channel interpretation schemes have been experimentally evaluated under different environmental conditions contributing to loss, e.g., mobility, interference, path-loss and multipath [54]. While convenient for practical deployment, loss-

triggered schemes, compared to SNR-triggered, have lower performance. Especially under low coherence time conditions, remarkable performance degradation and underselection problem in loss-triggered strategies are observed. On the other hand, SNR-triggered schemes, in spite being more robust, suffer from an "overselection" problem under fast-fading environments due to the false derivation of environment specific SNR-BER relationship, hence require training and calibration.

Additionally, losses on account of interference should be distinguishable from failures caused by channel quality variations. As pointed in [55], resource adaptation against interference does nothing but worsen the problem, to fight against this issue, *exponential-backoff* like structures might be preferable. In loss-triggered schemes, it is almost impossible to determine the source of the failure, while SNR-triggered schemes might develop such mechanisms. Furthermore, some other interpretations up to the physical layer (PHY) abstractions, as proposed in [55], could also resolve the issue.

Besides from these concerns, there are some additional considerations specific to the ambient energy scavenging transmitters and we cover two of them, harvester and battery related matters, in the next two subsections.

4.1.4 Energy Storage

Usually, energy harvesting transmitters are equipped with a rechargeable battery. Especially for the architectures where adaptation schemes would apply, perhaps the most crucial design concern is the choice of energy storage unit [57]. On the whole, two types of storage stands out in view of rechargeable transmitter design: ultracapacitors and batteries. Although the choice may vary depending on the application, several studies have found NiMH batteries as the best fit to physical design [57, 58].

As regards resource management, this design preference might have significant effects on the adaptation structure. Firstly, recharge efficiency of the battery would be amongst the resource allocation concerns. As opposed to the idealized fully efficient recharge process assumption in many analytical models, harvested energy cannot be stored in lossless manner, i.e., NiMH batteries have approximately 66% charge efficiency. Likewise, battery leakage is another source of inefficiency. Even in the absence of any energy consumption activity, some amount

of energy is lost due to a constant current leakage. However, the affect of this waste is not as severe as charging inefficiency and might be ignored in many scenarios. Finally, constraints imposed by the battery capacity could be examined as discussed in several studies [7, 26, 27, 30]. However, working within a full-battery dynamic region, even in the consideration of battery aging due to charge-discharge cycles, does not seem likely to be encountered in many scenarios. Based on publicly available empirical measurements on NiMH AA batteries, for example, constraints imposed by the limited capacity battery model is not likely to be tight due to recharge rate of typical harvesters being too small with respect to the battery capacity.

4.1.5 Harvesting

Advances in integrated circuit manufacturing and micro electronics have facilitated several ambient energy harvesting techniques, such as thermal, solar, acoustic, RF, and vibration-based, that could be deployed on self-sustainable communication devices. Similar to energy storage unit, selection of harvester type is a major physical design concern and should be regarded by the allocation schemes, as well. Depending on the source of ambient energy, for instance, battery level control periods could be adjusted. Additionally, issues mentioned in the previous subsection should be considered along with the harvester type, since hastening or deferral of energy usage decision depends on recharge characteristics. To this end, a deeper understanding of harvesting process is necessary and convenient energy harvesting models might need to be developed based on the source of energy.

Next, a cross-layer design concern will be covered in the following subsection.

4.1.6 Temporal Scaling

Processing operations on each layer are completed within different time scales. As an example, decoding algorithms generally take the longest durations among all processes. To coordinate the overall system operation, temporal scaling implications among and within layers should be regarded. In our case, power adaptation schemes, just like other activities, impose a processing cost. Additionally, the process comprises miscellaneous calculations involving inputs exported from different layers. Consequently, such interactions and dependence between network layers should carefully be examined and corresponding coordination

requirements need to be met. For instance, on medium access layer (MAC), timeout and inter-frame space durations might need to be adjusted, especially for the bidirectional transmission links, depending on the additional processing burden of the allocation scheme. Furthermore, additional adaptations might be essential, in case the processing duration varies in different scenarios.

4.1.7 Complexity

Last practicality concern to be considered in this section is the computational complexity of allocation schemes. As a matter of fact, complexity issue might be the most prominent concern by means of implementability determination. Excessively complex computations performed to pick a power/rate pair may defy the purpose of the adaptive scheme, as it will deem real-time adaptation difficult if not impossible, while the energy spent on computation may overshadow the energy savings from transmission. Needless to say, the policy should be implementable, regarding memory and processing capabilities of the hardware. Furthermore, interactions with other protocols also need to be taken into account to maintain overall system coordination. As discussed in the previous subsection, additional processing durations might violate system operation, unless necessary precautions are taken. Thus, implications of complexity burden within temporal scale need carefully be addressed.

4.2 Energy Conservation Intuitions

The ultimate goal of this chapter is to produce an implementable and efficient transmission scheme. In this context, regarding the practicality considerations discussed in the previous section, we aim to design and develop a novel algorithm. Before beginning the introduction of proposed allocation scheme, we first remark the basic intuitions of the algorithm. Firstly, it should be noted that efficient energy usage has been chosen as the primal goal of the design. Thus, intuitions to be listed within the section are energy-efficiency oriented.

4.2.1 Transmit Power Reduction

The first intuition that the algorithm makes use of is the most trivial and effective conservation mechanism, transmit power reduction. At the cost of delay or reliability, it is possible to transmit the same amount of information with a lower energy consumption. Specifically, by adjusting transmit power, the same amount of data can be transferred with the same transmission rate or reliability (BER) at the expense of a lower delivery rate or increased delay, respectively. Please note that, as the energy conservation and efficiency has been thought as the most significant priority, the setting should have delay or reliability tolerances. In our case, we will restrict maximum transmission power levels based on operation mode, correspondingly force algorithm to specify lower transmission rates, implying communication system could operate within some delay tolerance.

4.2.2 Avoidance of Idleness

In general, network architectures are based on packet-based transmission in modern communication systems. Rather than transmitting information as a series of data, through packet switched networks, communication medium can be more efficiently shared among users. In a packet switched network, however, information bits become available at different times during the course of transmission. By means of energy-efficiency, the arrival process of information poses interesting features into the scheduling schemes [20, 21, 22, 23, 24].

In the context of our study, energy efficiency could be improved by preventing buffer emptiness. As verified by the offline scheduling analysis in the previous chapter, hurrying on transmission within *low-load* buffer regions doesn't help conservation of energy. On the contrary, for the communication systems having a monotonically increasing energy per bit-transmission rate characteristics, it is possible to communicate more efficiently by lowering transmission rate, and thus avoiding transmission idleness as much as possible [20]. Even though this strategy might increase the delay cost per packet, overall transmission latency doesn't change.

4.2.3 Channel Adaptation

Particularly on wireless links, efficient energy usage might be improved by adapting to the timely variations of channel as discussed in several studies [7, 15, 22, 31, 56] and analytical investigation part of this thesis. On the observation of numerical analysis in Chapter 3, it could be noted that changes in channel quality have a strong influence on the allocation structure. Our intuition to conserve energy regarding this subject basically stems from the idea that, keeping the transmission rate constant, it is possible to achieve the same reliability level with a lower transmission power on high quality link instances. Thus, the transmission strategy involves utilizing good channel states more effectively, conserving more energy, and deferring transmission on poor quality link instances. Through this transmit power adaptation scheme, it could be noticed that we use a technique similar to truncated channel inversion. However, the idea behind of technique is different. While truncated channel inversion aims to maintain a constant data rate in all fading conditions, our scheme makes transmit power decision after the rate choice, and thus aim to reduce energy usage in accordance with the reliability requirement. This issue will further be discussed in the next section.

4.2.4 Battery Adjustment

As reviewed in Section 4.1, battery inefficiency should be taken into consideration. To this end, consumption of energy before storage is a potential solution. Even though the scheme might not be practical in all settings and cases, i.e., deficiency in hardware infrastructure or operation under high recharge rate, remarkable conservation gains might be obtained in systems where direct consumption without storage strategy is applicable. However, as discussed earlier, speeding up transmission might be disadvantageous at the same time. Particularly within low battery operation regions, a more special attention on energy consumption should be paid since, storage might become a priority in such situations. In overall, the tradeoff between battery and rate level oriented inefficiencies must be balanced based on system conditions. Our strategy regarding this subject will be detailed in the following section.

4.3 The Algorithm

Up to this point, the thesis has focused on analytical models of scheduling as well as practicality considerations to form basic intuitions and insights to develop a final successful outcome. The rest will consider the design and development of this end product, an implementable novel transmission strategy. We begin with the general outline of the design of our proposed scheme.

As noted in Section 4.2, the algorithm ultimately aims an energy-efficient transmission structure. In this manner, energy conservation intuitions mentioned earlier form the basis of the architecture. The simple tools at hand are, basically, adjusting transmit power and rate, within certain limitations, in response to the data load as well as the battery state and the channel conditions. In addition, we will consider slot length (a slot is an interval during which the buffer is allowed to accept incoming data packets). Once per slot, the data buffer as well as the battery state is checked, and a transmission decision is made. We will consider slot length as a variable. Compared to other parameters, this is a more readily tunable parameter in a practical system, and hence will be a poignant point of this algorithm.

Firstly, the algorithm regards battery level changes and determine transmission strategy accordingly. Depending on the battery status, one of the three different modes of operation¹ takes place, hence we call the scheme as *TriMod*.

1. **Generous Mode:** This mode is characterized by aggressive operation and takes place during relatively high battery level state. Correspondingly, maximum allowable power level is set to the highest and initial slot size to the minimum. Through this strategy, we aim to reduce delay cost per packet and prevent losses due to battery imperfection. The basic idea behind this decision is that, as the operation is less energy critical within the neighbourhood of full battery region, the scheme works based on a more performance-oriented layout.
2. **Conservative Mode:** In contrast to the generous, the conservative mode expects a low load, which means checking the buffer less often (i.e., a large slot size), and has less tendency to transmit due to the lower maximum admissible transmit power. In

¹ We consider three operation modes to cover the two extreme cases and the moderate between these two. However, fundamentally following the same idea, the number might be increased.

addition to the transmit power restriction, transferring information after a longer data accumulation course contributes energy conservation as well, since it is possible to keep rate level constant during a longer period of time. As the energy conservation and storage become the most significant priorities for the systems suffering energy shortage, this mode of operation emerges under low-battery conditions.

3. **Moderate Mode:** In between the two extremes, we allow another, moderate, mode. Within this transmission plan, upper and lower bounds on transmit power and slot length levels, respectively, are set to the intermediate values as compared to generous and conservative modes.

It should be emphasized that, to prevent instability, transitions between two modes, e.g., from generous to moderate and moderate to generous mode, should occur at carefully selected boundaries. As an example, if the switch from generous to moderate mode happens at 70% of rated battery capacity, reverse transition should occur at a different battery level, 80% for instance. By selecting, particularly, higher boundary levels for the transitions towards generous mode, and lower values vice versa, recharge rate tendency, i.e., whether the battery tends to get charged or discharged, is also taken into account as another alteration criterion between operation modes. Furthermore, the scheme could easily be implemented by measuring battery voltage level periodically through the use of low power battery monitor ICs.

Broadly speaking, the operation mode is chosen based on the current state and tendency of the battery level. In each mode, there is a predefined maximum allowable power level² and an initial slot length assignment. Primarily, the policy decides a transmission rate among up to these parameters and desired packet error rate (PER) tolerance. Specifically, the rate allocation strategy is based on the observation that, there exist a threshold channel gain level, satisfying the target reliability, for each achievable transmission rate³ and power level. In this manner, we first determine boundary channel gains for each admissible transmit power and achievable rate. Afterwards, the rate decision is given as follows:

$$r = \min \left\{ \left\lceil \frac{q(t)}{L} \right\rceil, \max \{ r_i \mid h \geq \gamma^i, i = 1, 2, \dots, k \} \right\} \quad (4.1)$$

² By restricting the transmit power, limitation imposed by linear region of power amplifiers is taken into account.

³ We assume a k -element set of discrete rates

In equation (4.1), $q(t)$ and L denote the number of data bits accumulated in the buffer by time t and the slot size, respectively. h is the square of the most current channel gain. In addition, r_i and γ^i represent, in turn, i^{th} achievable rate and corresponding threshold channel gain. Depending on the current fade level, and operation mode, the set of data rates satisfying PER are obtained. Among this set, maximum rate value is chosen. Afterwards, another data rate based on the current slot length and data buffer is determined by the policy. Between these two, the minimum value is assigned as the transmission rate of the upcoming slot. The fundamental idea behind this decision is that, transmission with a rate beyond either current channel state or data buffer allowance, violates PER tolerance or cause idleness of the system, respectively. Consequently, the limitations of channel and data buffer are taken into account. Moreover, we propose another mechanism to avoid transmission idleness. During the control of data buffer step, the policy checks if there is enough data in the buffer to ensure nonstop transmission within the slot. If not, the policy decides to double slot length so as to accumulate more data in the buffer.

After the decision of transmission rate, the policy determines transmission power value based on the PER requirement. Given a transmission rate, the minimum possible transmission power value satisfying PER requirement is chosen as follows:

$$P = \frac{SNR(r) \cdot N}{h} \quad (4.2)$$

In equation (4.2), $SNR(r)$ is a function returning the threshold SNR value corresponding to a given rate, r , and the desired PER. Additionally, N and \sqrt{s} denote the noise power and channel gain, respectively. Observe that, transmission power value varies inversely proportional to the channel gain and transmission is deferred in case channel gain being lower than threshold corresponding to minimum achievable data rate. Along these lines, the power allocation scheme resembles truncated channel inversion idea [59].

$$\frac{P(h)}{\bar{P}} = \begin{cases} \frac{\sigma}{h} & \text{if } h > \gamma_0 \\ 0 & \text{otherwise} \end{cases} \quad (4.3)$$

As noted in equation (4.7), truncated channel inversion strategy assigns power levels inversely proportional to the channel state when fading is above a cutoff fade depth, γ_0 . Respecting the average power constraint, \bar{P} , a constant received SNR of σ is intended. TriMod

scheme, however, prioritizes rate allocation and power assignment comes after this decision. Note that, proposed scheme does not intend to achieve a constant SNR level at the receiver side. In addition, it respects a predefined PER requirement, meaning transmission power is lower bounded once the rate decision is made. Thus, channel inversion takes place within a limited operation region and power allocation shall be regarded as a compensation of energy consumption for the rate assignment.

Not necessarily at the end of each time slot, the policy periodically checks the battery state and updates operation mode. Indeed, this interval shall be determined by the characteristics of harvesting process. Furthermore, adaptation of the buffer checking period could be considered in order to reduce the cost of battery monitoring ICs. Especially for the predictable harvesting sources, solar for instance, such schemes could be worth deploying. The operation of the policy is summarized by the following flowchart in Fig 4.1.

This completes the general outline of the algorithm. However, there are still some confusing points to be clarified. Particularly, we have not given any details regarding how the scheme obtains information on channel gain. Actually, as mentioned earlier, channel gain estimation is a difficult problem and SNR-based rate adaptation scheme has not been commonly implemented yet. However, the heuristic is still applicable through the usage of some cross-layer adaptation techniques [55, 54]. Especially, the *SoftRate* mechanism proposed in [55] is quite convenient for our purposes and the basic layout of the strategy will be summarized here to provide integrity. Before that, a simpler but less accurate way to resolve the problem is worth mentioning. Many of the receivers today, e.g., 802.11 devices, are capable of estimating received SNR. These measurements could be sent back to the transmitter over a feedback channel to predict current channel gain. However, this solution strategy suffers from not being able to detect interference and environmental dependence of SNR-PER characteristics.

On the other hand, *SoftRate* makes use of per bit confidences, "*SoftPHY* hints", exported by PHY to compute interference-free bit error rate (BER) estimates. As a first step, the algorithm calculates BER corresponding to current transmission rate. Considering a frame transmission, where $x_k, k = 1 \dots N$, are the input bits to the encoder and \mathbf{r} denote the corresponding received signal at the decoder, *SoftPHY* hints, s_k , are defined as follows:

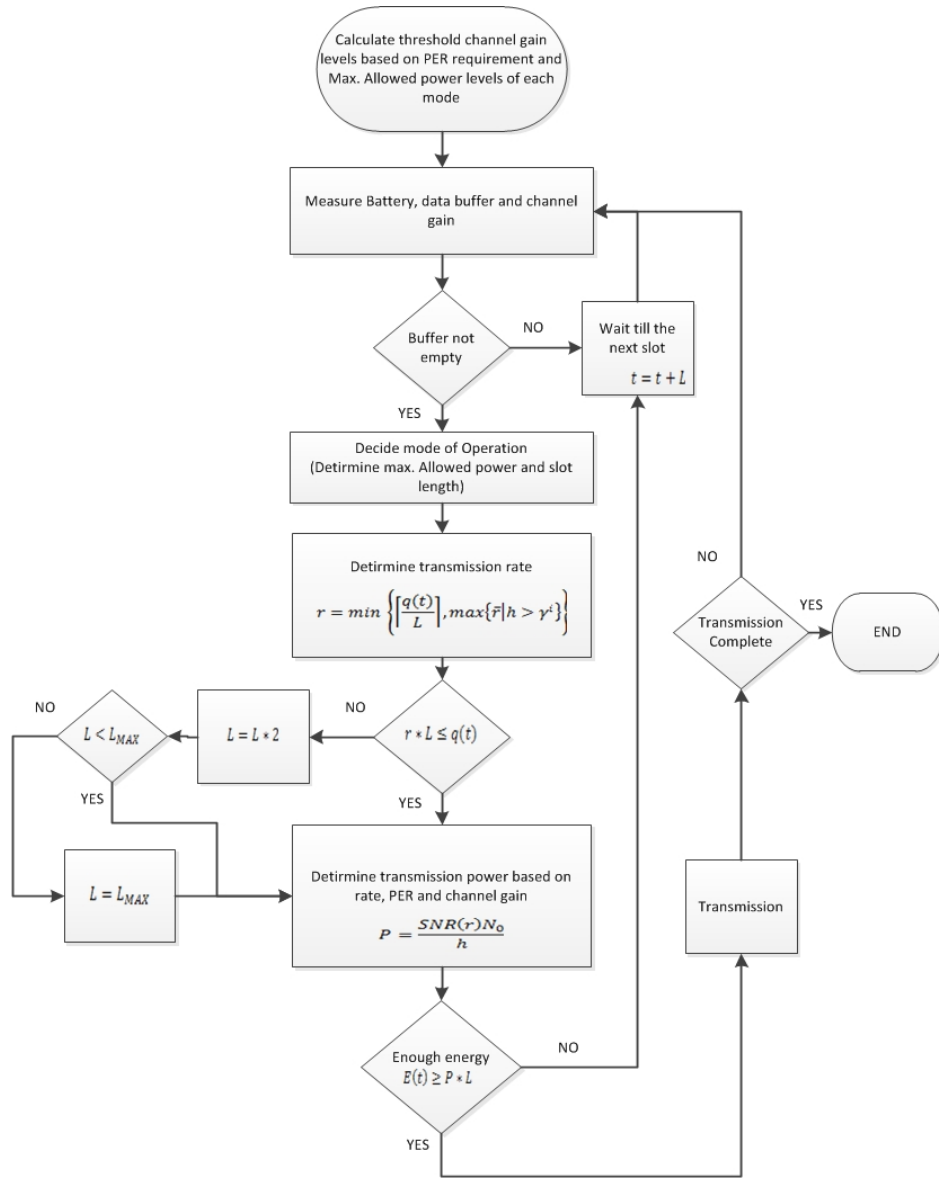


Figure 4.1: Flow graph representation of the TriMod algorithm

$$s_k = \left| \log \frac{P(x_k = 1 | \mathbf{r})}{P(x_k = 0 | \mathbf{r})} \right| \quad (4.4)$$

$$= \log \frac{P(x_k = y_k | \mathbf{r})}{P(x_k \neq y_k | \mathbf{r})} = \log \frac{1 - p_k}{p_k} \quad (4.5)$$

Solving for p_k yields:

$$p_k = \frac{1}{1 + e^{s_k}} \quad (4.6)$$

Here, equation (4.5) is obtained on the assumption that bit error event is always less likely, i.e., $p_k \leq 0.5$ and y_k denotes the corresponding output from the decoder to the x_k . Averaging over all k bits correspond to the most recent average BER of the transmission rate. Regarding bit rate adaptation, however, interference sourced errors might cause serious performance degradation. In this manner, SoftRate employs a heuristic to excise the fractions of the frame subject to strong interference and average is taken over interference-free portion. Furthermore, the protocol estimates corresponding error rates of the remaining achievable rates based on monotonically increasing nature of BER-data rate relationship. As regards TriMod, calculated BER values for each transmission rate could be utilized to make the rate decision. To this end, first a few packets within a slot should be transmitted with the maximum allowable power level, since the threshold values in (4.1) are obtained based on permissible power levels of each mode. Afterwards, transmission power could be reduced based on the predicted PER of the transmission rate and SNR-PER observations.

As can be noticed, integrating SoftRate algorithm into TriMod is not an easy task and cost additional inefficiencies together with the complexity burden. Specifically regarding TriMod, which scheme to employ for obtaining channel side information is an environment and application specific decision. Intuitively, simpler structures to interpret the channel state could be more favourable under slowly varying channel and low-interference regime conditions, while algorithms like SoftRate might need to be deployed under the opposite circumstances. Between these two extremes, however, appropriate decision is not too obvious to make and experimental evaluations are need to be performed. Such analysis has not been made in the scope of this thesis, but may be considered in future work.

Finally, cross-layer implications on MAC shall be considered. Although, fundamental MAC structure of current standards are suitable to be integrated with TriMod, there are some minor issues to be handled. Firstly, timeout, backoff and synchronization related durations of the

random access scheme should be rearranged regarding temporal scale effects. In addition, how to inform the transmitter about the channel state should be decided. Especially, for the schemes employing a four-way handshake mechanism, appending a field containing SNR or BER information for instance, in the header of the clear to send (CTS) message is a possible solution.

4.4 IEEE 802.11

Before beginning the analysis of proposed scheme, a brief introduction to IEEE 802.11 specification will be given, hence the numerical studies and implementation experiment will be based on this setting. Since the first announcement of the standard in 1997, there has been several extensions, among which 802.11 b/g/n versions have become widespread. In our study, the 802.11g standard will be considered, since it is the most current SISO extension among these extensions.⁴ Specifically, the standard prescribes the usage of 64 OFDM subcarriers within 2.4 GHz frequency band and supports transmission over 8 different data rates [60]. In Table 4.1, these rates along with the corresponding PHY settings are listed.

Table 4.1: IEEE 802.11g data rates, modulation modes and coding rates

No.	Modulation scheme	Code rate	Data rate
1	BPSK	$\frac{1}{2}$	6 Mb/s
2	BPSK	$\frac{3}{4}$	9 Mb/s
3	QPSK	$\frac{1}{2}$	12 Mb/s
4	QPSK	$\frac{3}{4}$	18 Mb/s
5	16-QAM	$\frac{1}{2}$	24 Mb/s
6	16-QAM	$\frac{3}{4}$	36 Mb/s
7	64-QAM	$\frac{2}{3}$	48 Mb/s
8	64-QAM	$\frac{3}{4}$	54 Mb/s

In this context, several rate adaptation algorithms [61, 62, 63, 64, 65] have been proposed regarding the PHY of the standard. Furthermore, a few have been employed for commercial use. Among these adaptation schemes, Auto Rate Fallback (ARF) and Receiver Based Auto Rate (RBAR) are the most widely-used algorithms. In general, these methods adapt transmission parameters based on channel conditions in order to maximize long-term throughput.

⁴ Even though the algorithm is also applicable on MIMO systems, to provide compatibility of implementation demo with numerical experiments, analysis will be conducted over a SISO scheme.

Particularly, RBAR is an SNR-based mechanism and achieves better performance in many cases as experimented in [66]. However, ARF, originally developed for Lucent Technologies' WaveLAN-II WLAN devices, has become the most widely accepted scheme in the 802.11 market. Most of the success and popularity of this algorithm comes from being structured in an easily applicable way and being compatible with the specification. Without requiring any additional design burden and practicality concern, ARF could be integrated into any readily available 802.11 standard.

Basically, ARF keeps track of the consecutive ACK messages and timeouts. During the adaptation process, transitions occur between the closest achievable rates. In particular, 2 sequential ACK losses imply reduction of rate to the nearest lower value. Adversely, transmission rate is increased to the next higher one in case the number of successive ACK receptions reach 10 or a predetermined timer expires without any ACK losses. On the other hand, RBAR scheme prescribes the use of RTS/CTS mechanism to adapt timely variations of channel. Based on the calculations over RTS messages, receiver informs the transmitter via CTS packets. Afterwards, rate decision is made comparing the SNR value with the thresholds corresponding to the priori channel model. Especially, due to the requirement to change interpretation and format of the RTS/CTS frames, the scheme has not been employed by any off-the-shelf 802.11 device. However, through the use of *cognitive radio* and *software defined radio* ideas, practicality and efficiency of the scheme has been shown [66], implying the promising employment potential of SNR-based adaptation schemes in the market.

When it comes to the power management, today's WLAN energy-conservation technologies do not go any further than sleep-wake scheduling. In fact, most 802.11 devices operate over Constant Awake Mode (CAM) due to the performance reduction concerns in terms of throughput. Moreover, WLANs today are being powered by constant AC sources and energy efficiency doesn't contribute performance enhancement. In our case, however, efficient use of energy is the primal focus and have strong influences on long-term performance.

4.5 Optimal Offline Schedule

In Chapter 2, recent literature regarding resource allocation problems from the energy scavenging communication systems point of view was summarized. None of these studies, how-

ever, has considered an implementation approach to the problem, and thus cannot provide useful benchmark algorithms for the performance evaluation of TriMod scheme.

In the following section, numerical analysis of the proposed scheme will be given by comparisons to the optimal offline solution. Offline analysis of scheduling problems, as stated earlier, provide strict performance boundaries and useful benchmarks to heuristics. Although the offline formulation in section 3.1.3 is a good approximation, discretized nature of achievable data rate and power set has not been addressed. Therefore, another offline scheduling problem is defined in Pr. 5, taking the implementability concerns discussed in section 4.1 into account. Before beginning to the formal definition, we first define a rectifier function $[x]^+$ as follows:

$$[x]^+ = \begin{cases} x & x \geq 0 \\ 0 & x < 0 \end{cases}$$

The formulation is built based on the physical practicality concerns reviewed throughout the Chapter, i.e., discrete rate and power set, battery inefficiency and reliability requirement. As the proposed scheme is developed based on energy-efficiency concerns, its objective is to minimize overall energy consumption during the transmission course of packets accumulated by time T .

Problem 5 Energy Consumption Minimization in a Discrete Rate and Power Transmission With Battery Inefficiencies:

$$\text{Minimize: } E^c(T) = \sum_{i=1}^L P_i \xi_i + \eta \sum_{i=1}^L \left[\frac{E_i}{\xi_i} - P_i \right]^+ \xi_i$$

$$\text{subject to: } \sum_{i=1}^n P_i \xi_i + \eta \sum_{i=1}^n \left[\frac{E_i}{\xi_i} - P_i \right]^+ \xi_i \leq \sum_{i=1}^n E_i \quad (4.7)$$

$$\sum_{i=1}^n r_i \xi_i \leq \sum_{i=1}^n B_i \quad (4.8)$$

$$\frac{P_n S_n}{N} \geq \text{SNR}(r_n) \quad (4.9)$$

$$\sum_{i=1}^L r_i \xi_i = \sum_{i=1}^L B_i \quad (4.10)$$

where $P_i \in [P^1, P^2, \dots, P^m]$, $r_i \in [r^1, r^2, \dots, r^k]$ and $n \in [1, 2, \dots, L]$

In Pr. 5, it is assumed that there exist L distinct epochs by T , $\sum_{i=1}^L \xi_i = T$, and battery gets charged according to an inefficiency constant, $\eta < 1$. Among an m and k element sets of transmission power and rate, the transmitter is expected to make an assignment for each epoch such that all the accumulated data is transmitted by T (4.10). During the assignment, the transmitter is required to respect energy and data causality constraints in (4.7) and (4.8), along with the error tolerability (4.9). By respecting to the channel gain changes, i.e., $\sqrt{s_n}$ denoting the channel gain during epoch n , desired PER requirement should be satisfied for each packet transmission. Accordingly, $SNR(r)$ function returns the corresponding SNR value to the desired PER and data rate r . In addition to the energy used for transmission activities, energy lost due to the recharge inefficiency is also considered. Specifically, in case instantaneous recharge rate exceeds transmission power, η fraction of remaining energy gets stored in the battery.

Solution techniques discussed within Chapter 3 do not help to the solution of Pr. 5, since the objective involves discontinuities and the formulation does not fulfil the convexity requirements. However, it is now possible to obtain an optimal assignment through exhaustive search techniques. Due to the limited number of possibilities on rate and power assignment, i.e., discrete transmission rate and power set, solution of Pr. 5 can be attained by trials of every single possibility. Although this solution technique suffers from high complexity issues, it helps provide benchmarks at least in the short-term, i.e., Fig. 4.5 and Fig. 4.6.

Considering the structure of IEEE 802.11 specification and optimal offline solution, performance evaluation of the proposed scheme will be covered in the following section.

4.6 Numerical Study

The scope of this section is the performance evaluation of TriMod algorithm under 802.11g PHY by numerical comparisons in MATLAB. For this purpose, RBAR and optimal offline solution schemes are chosen as the benchmarks. In addition, achievable transmit power levels are assumed to be within a finite element set, i.e., $\{3, 5, 7, 10, 12, 15dBm\}$, along with the discrete set of data rates specified in 802.11g. This assumption involves practicality concerns as mentioned in Section 4.1.2 and facilitates attainability of optimal offline solution through brute-force search technique. However, as the computational complexity of the search tech-

nique is exponential with the number of epochs, it is only possible to derive optimal solution of a finite-horizon scheduling problem formed by a few epochs. Fortunately, comparisons on the behavioural structure are still possible. In overall, TriMod will be examined by comparison to the RBAR scheme in terms of energy efficiency-delay performance and optimal offline solution by means of structural similarities.

Before we begin analysis, background details of the numerical experiments shall be introduced. Firstly, we consider a subset of 802.11g rates and the threshold SNR values corresponding to a PER of 10^{-2} as specified in Table 4.2 [67].

Table 4.2: A subset of 802.11g data rates, corresponding threshold and maximum throughput values

No.	Data Rate	SNR (PER:10e-2)	Max. Throughput
1	6 Mb/s	1.2 dB	5.0
2	12 Mb/s	4.3 dB	8.4
3	24 Mb/s	10.0 dB	13.0
4	36 Mb/s	13.2 dB	15.9
5	48 Mb/s	15.5 dB	17.9
6	54 Mb/s	18.9 dB	18.5

Data and energy arrivals are modelled as Poisson random processes with arrival rates λ_d and λ_e , respectively. In addition, packet lengths and recharge rates are determined by random quantities relative to the actual 802.11 packet sizes and empirical solar panel measurements, accordingly. In order to take the battery inefficiencies into account, only 66% of the input energy is assumed to be stored. Moreover, to let the algorithm to change some states within a reasonable time, battery size is chosen to be 907,2 mJ which is 10^4 times less than a standard AA battery and battery level is assumed to be at 700,0 mJ at the beginning. Channel is modelled as Rayleigh fading channel and coherence time is chosen predicated on the ISM band measurements in a typical office environment [66], i.e., 100 ms. Data packets are allowed to arrive until the end of the 10^6 milliseconds. Depending on the operation mode initial slot size assignments are set to 2, 8 and 16 ms accordingly. On the other hand, admissible transmit power levels are restricted by 5, 10 and 15 dBm values, corresponding to conservative, moderate and generous modes respectively. As noted in the previous section, however, transmit power doesn't vary in conventional WLAN devices. Therefore, transmit power level in each RBAR run is assumed to be constant at 15 dBm, which is approximately the case in many

802.11 transmitters, and RBAR is thought to operate every 2 ms. Finally, transitions between operation modes are planned to occur at 30% and 80% of rated battery regime correspondingly for the transitions from moderate mode to conservative and generous modes. Likewise, operation is assumed to vary from conservative and generous modes to moderate at the borderline of 40% and 70% of battery capacity, respectively. Under these circumstances, a few numerical experimentations were conducted. We shall begin with, performance comparison of RBAR and TriMod schemes. Before that, a final detail about the analysis should be emphasized. In each run, the experiment is terminated if either both policies complete transmission of data arrived by 10^6 ms without depleting the battery or one of the policies complete transmission at some instant T and the other cannot due to battery depletion by T . In view of the foregoing, efficacy is defined as the number of transmitted bits per unit energy consumption and chosen as the primary performance criterion.

Firstly, the allocation schemes are compared for different values of data arrival rates and the results are depicted in Fig. 4.2. For this experiment, λ_e is set to 0.02, corresponding to average interarrival duration of 50 ms, and λ_d is ranged from 0.1 to 1.0 with an increment factor of 0.1. In each case, TriMod completes transmission of all the bits, while RBAR suffers from battery depletion, except for the case where λ_d is 0.1, and transmits just a portion of accumulated data. As clear from the figure, efficacy of TriMod is much superior to that of RBAR and gets better under heavier load. When it comes to the delay per packet, RBAR scheme performs better than TriMod when data arrival rate is 0.1. However, for the rest of experiments, delay performance of RBAR dramatically worsens due to running out of battery. The policy needs to wait until enough energy is harvested in case of battery depletion. Consequently, transmission of accumulated packets in data buffer occur with an enormous amount of latency. Under heavy loads, this issue may even result unstable system operation with respect to the queue state. On the other hand, TriMod takes battery level into account and prevents battery depletion by deferring transmission for the battery critical cases. In addition to the outstanding energy efficiency achievement, the policy accomplishes a reasonable delay per packet performance.

The same experiment is repeated by doubling the initial slot length assignments in moderate and conservative modes. The second set of data given in Fig. 4.2 shows the further efficacy enhancement potential by increasing slot sizes. From these set of evaluations it has been observed that, improvement of efficacy by playing with slot sizes comes at a cost of increased latency. In particular, by doubling the slot length durations within moderate and conservative

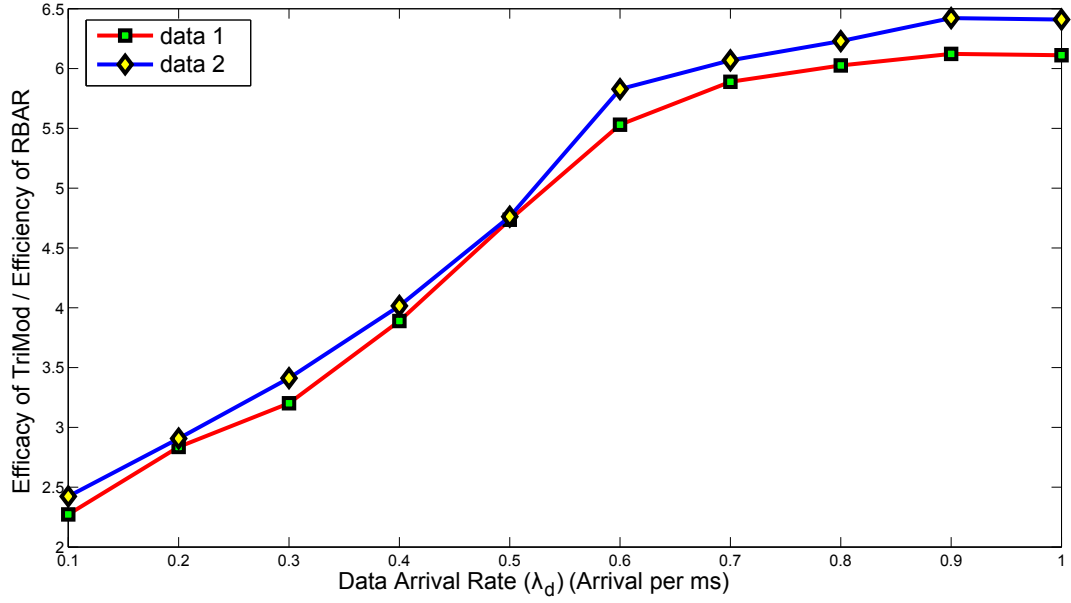


Figure 4.2: TriMod vs RBAR for different data arrival rates. First set of data is obtained for the initial slot length values of 8 and 16 ms corresponding to generous and conservative modes, respectively. The second set of data is obtained under doubled initial slot length assignment for conservative and generous modes.

modes, average delay per packet performance of TriMod scheme is observed to degrade with an approximate degree of 55%. Consequently, the first slot length setting seems more reasonable considering the values of interest. As a matter of fact, slot size assignments corresponding to each operation mode should be based on delay tolerance and arrival characteristics of the system. Considering the nature of conflict between energy efficiency-delay performance and system requirements, optimal slot durations can be chosen.

Next, allocations for different energy arrival rate values are compared. Specifically, λ_e is varied within the set of $\{0.001, 0.005, 0.01, 0.02, 0.05, 0.1\}$ and λ_d is set to 0.3. Once more, evaluation results are shown in Fig. 4.3 by means of efficacy. As the operation tends to be more conservative within low rate harvesting regimes in TriMod policy, efficient use of energy increases, at a price of higher latency performance, as λ_e decreases. The examination has also repeated for the increased slot length durations. Corresponding outcome is denoted by the second set of data in Fig. 4.3, which supports the previous observation on energy efficiency-delay tradeoff.

In Fig. 4.4, evaluation results under different initial battery levels are depicted. By keeping the arrival rates, λ_e and λ_d , constant, efficient use of energy performances regarding TriMod

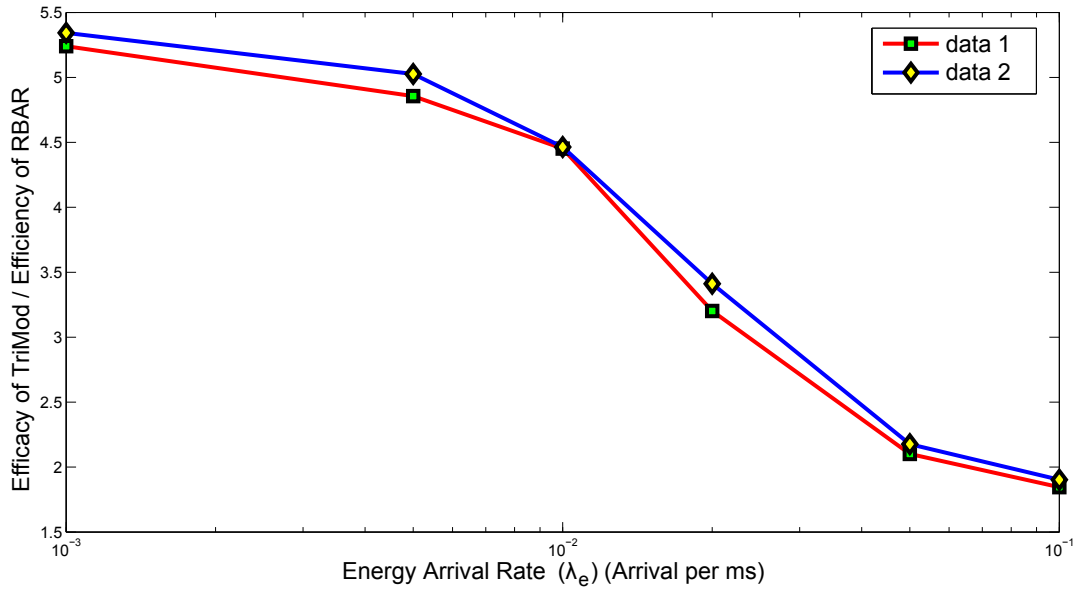


Figure 4.3: TriMod vs RBAR for different energy arrival rates. First set of data is obtained for the initial slot length values of 8 and 16 ms corresponding to generous and conservative modes, respectively. The second set of data is obtained under doubled initial slot length assignment for conservative and generous modes.

and RBAR policies were examined. The first set of data in the figure was obtained by varying initial battery levels of both policies, while RBAR scheme's initial storage level was kept constant during the second experiment. Firstly, it should be noted that, proposed heuristic, in contrast to the RBAR, completes transmission of all information bits in each run. Even under initial low battery disadvantage, TriMod transmits more data while consuming less energy. The policy adapts itself to the battery state and compensates the initial low battery handicap. Furthermore, it could be observed from this experiment that energy conservation property of TriMod policy stands out under battery critical cases. So far, conducted experiments prove the crucial need for novel adaptation techniques in ambient energy scavenging communication systems. At first sight, more aggressive policies might seem more favourable by means of performance concerns. Due to wasteful transmission characteristics, however, such policies suffer from energy shortage in long term and result irretrievable performance degradation. Concisely, it could be concluded that, besides from energy efficiency, throughput and delay characteristics have strong dependence on energy conservation.

As a matter of fact, RBAR scheme has not been developed considering energy harvesting transmission systems, and thus it could be more reasonable to compare the proposed scheme

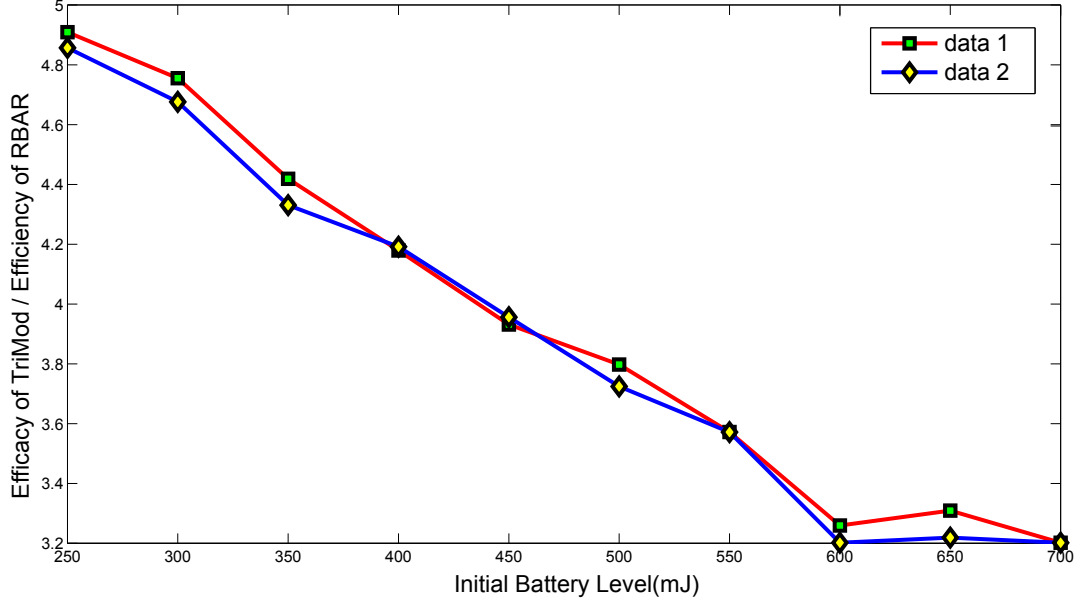


Figure 4.4: TriMod vs RBAR for different initial battery levels. First set of data is obtained by varying initial battery levels of each policy, while the second is obtained by changing just the initial battery level of the transmitter where TriMod operates.

with other policies having similar concerns and goals. However, to the best of our knowledge, this is the first study aiming development of practical schemes for rechargeable transmitters with concave energy per bit-rate characteristics. As noted in previous chapters, offline analysis can provide useful benchmarks. As a restricted achievable transmission power and rate set is considered, optimal offline solution could be obtained through brute-force search technique. In the following two experiments, in addition to the RBAR scheme, proposed heuristic will be compared to the optimal offline solution. Specifically by examining the resource allocation on each slot, structure of the policy will be investigated from a deeper perspective.

Firstly, consider the event sequence depicted in Fig. 4.5. For this event set, transmission the deadline, by which all the accumulated data should be sent, is determined as $t = 3.7ms$. In addition to the achievable rate set of 802.11 g specification, transmit power levels are to be selected within the set of $\{3, 5, 7, 10, 12, 15\}$, implying 36 different power-rate assignment possibility during an epoch. Optimal policy is thought to be the one that transmits all the information bits till deadline by consuming minimum amount of energy.⁵ Under such an experiment setting, TriMod scheme is compared with offline optimal and RBAR. Please note

⁵ It is possible to make other optimality definitions with quite different objectives, such as average delay per packet or jitter minimization. In the sense of our investigation, however, selected criterion fits best.

that, computational complexity of brute-force search is exponential. In order to obtain the optimal solution for a 6 epoch transmission period, as in the example considered in Fig. 4.5, 6^{36} possible assignments must be computed. Thus, the search technique has practicable limitations and only a limited number of epochs could be considered for investigation purposes.

In this examination, battery is assumed to be discharged at the beginning and TriMod policy was operated over conservative mode, adapting to the battery, data queue and timely variations of channel in an epoch length scale. For the experimental setting of interest, the policy is observed to achieve optimal performance. By means of rate and power assignment, behaviour of TriMod policy depicted in Fig. 4.5 is the same with optimal policy's. Specifically for this experiment, RBAR completes transmission almost 1 ms before than TriMod. On the other hand, energy consumption of the policy is almost four times larger. Additionally, it is observed that TriMod doesn't achieve the optimal just for this experiment but also converges to the offline optimal under different settings, where deadline constraint is relatively high and channel is not dominated by deep fades.

Next, another experiment with similar events were conducted. In particular, durations are shortened to bring the deadline forward and force the algorithms to rush. Under such circumstances, conservative operation mode of TriMod policy couldn't complete the transmission till deadline but sent 91% of accumulated data. Thus, moderate operation mode is to be considered in comparisons. Before the details, it should be emphasized that TriMod policy achieves better efficacy performance, albeit not being able to complete the transmission. In summary, it could be concluded about the conservative operation of TriMod policy that, performance of the scheme is as successful as desired by means of energy efficacy.

In Fig. 4.6, transmission rate and power allocations of RBAR, TriMod and optimal policies are depicted. It could be observed from the figure that, RBAR completes the transmission first, next followed by order of TriMod and optimal, respectively. In addition, the similarity between the structure of moderate operation of TriMod and optimal policy might be easily noticed. Especially, rate allocations of the policies are quite alike. As a consequence of this structural similarity, moderate operation achieves 75% efficacy as compared to the optimal, while RBAR accomplishes just 25%. Moreover, stated analogy is observed to hold under various different experiment settings.

In a similar fashion, the policy has been evaluated more than a hundred times in short-term.

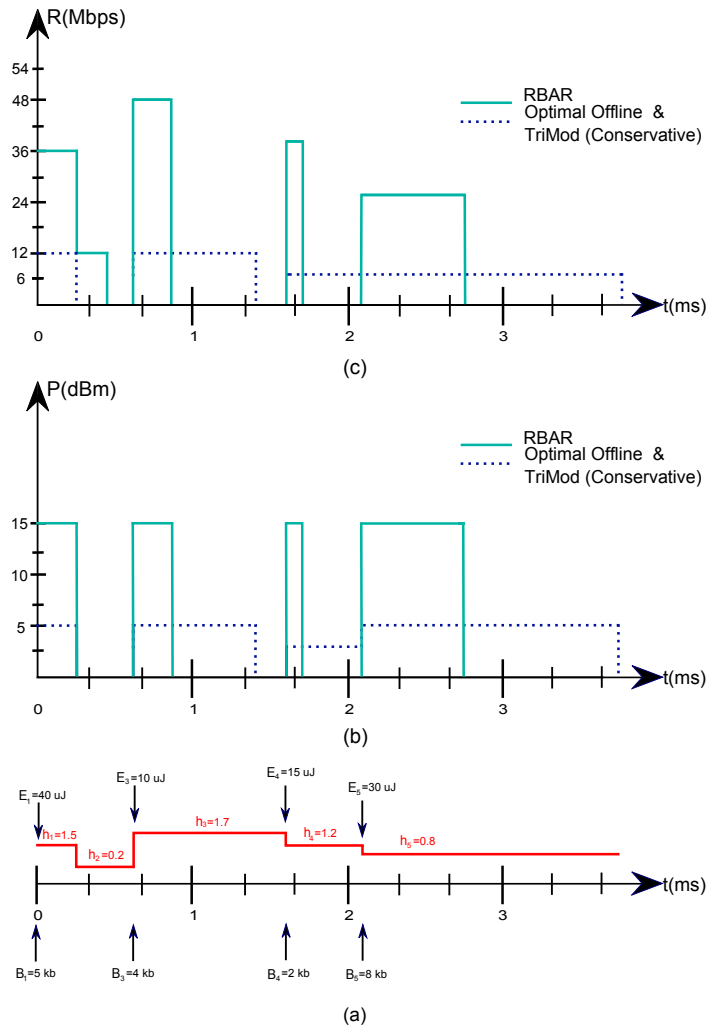


Figure 4.5: (a) Corresponding event setting used in the experiment. The squared channel gain in the i^{th} epoch is h_i , energy harvest amounts and arriving data are marked as E_i and B_i , respectively. (b) Power assignments in dBm. (c) Final rate schedule of the policies.

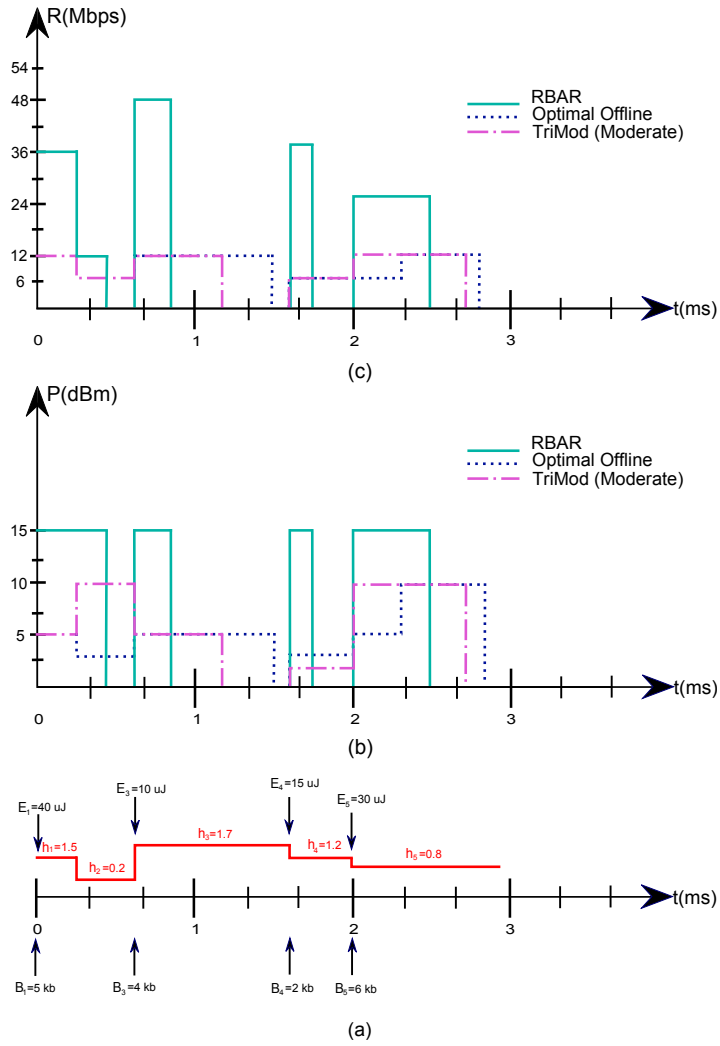


Figure 4.6: a) Corresponding event setting used in the experiment. The squared channel gain in the i^{th} epoch is h_i , energy harvest amounts and arriving data are marked as E_i and B_i , respectively. (b) Power assignments in dBm. (c) Final rate schedule of the policies.

At the end, it has been observed that, TriMod achieves approximately 85% efficacy in average as compared to the optimal. On the other hand, RBAR scheme, in average, could achieve just 17% efficacy as compared to the offline optimal.

In conclusion, fundamental observations of conducted experiments are as follows. Conventional transmission strategies cannot meet the requirements of rechargeable transmission systems. Additional considerations such as battery and recharge state are required to be taken into account. In comparison to the adaptation schemes in the literature, proposed allocation strategy is quite novel. Furthermore, as regards efficacy, the policy bears significant resemblance to the offline optimal by means of allocation structure.

4.7 Implementation Experiment

Finally, an implementation experiment, implying the practicality of the proposed scheme, has been done. The aim of the section is to realize crucial points of the TriMod algorithm over the specific hardware and development platforms. For this purpose, Software Defined Radio (SDR) approach will be used.

The SDR concept involves the implementation of conventional communication blocks by means of software on programmable digital platforms, such as personal computers (PC) [68]. The idea, proposed in [69], introduces flexible and reconfigurable radio devices and enhances the adaptive resource management schemes for communication systems. The basic concept comes from the idea that, depending on the current necessities of the system, user or application, available resources like spectrum band and energy could be used more efficiently. Furthermore, it might be possible to produce multifunctional communication devices, being able to operate over more than one protocols including PHY specifications and to build decentralized communication systems. Typically, software defined radio architectures consist of three main components, RF front end, analog-to-digital converter (ADC) or digital-to-analog converter (DAC) and processing unit, as depicted in Fig. 4.7. On the receive path, RF front-end demodulates the radio signals into an intermediate frequency (IF) and then ADC digitizes the analog signal through sampling and conversion. Finally, the raw data in digital form is processed, e.g., demodulation and decoding, on a PC or an embedded processor. Correspondingly, reverse operations are performed on the transmit path.

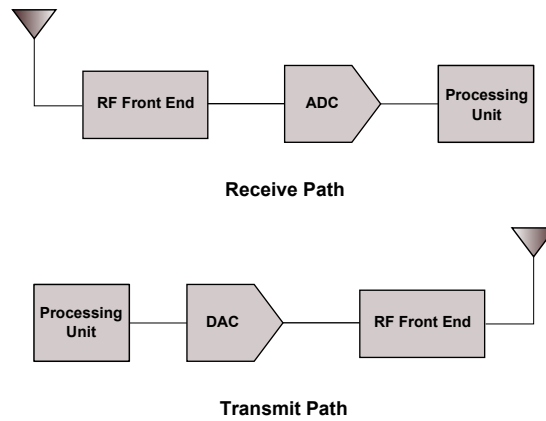


Figure 4.7: A typical software radio structure

The flexibility provided by software replacement of conventional processing approach, to perform signal processing on analog circuitry combined with digital design, is a revolution by means of design challenges.

4.7.1 GNU Radio

Recently, several SDR platforms, employed particularly for academic and teaching purposes, have come on the scene. GNU Radio [70], primarily using the Universal Serial Radio Peripheral (USRP) [71], is one the most popular among these frameworks. GNU Radio is an open source project and provides several signal processing libraries, which implement basic processes of a typical communication system, in addition to the tools for holding these processing blocks together. Specifically, a transmission architecture could be built over GNU Radio platform by implementing the corresponding signal processing blocks in C++⁶ and glueing each block in Python. Conceptually, this completes the construction of a flow graph and facilitates infinite stream of data processing on a typical PC. In the lower level of abstraction, actual implementation of a block is defined by the codes written in C++. Each signal processing block has attributes like number of inputs-outputs and type of the data to be processed. In the higher level, through the use of Python, each convenient block can be connected up to these attributes. Furthermore, in between these two layers, the framework makes use of a library called SWIG (Simplified Wrapper and Interface Generator) to integrate Python and

⁶ Most of the fundamental processing blocks have already been implemented in the latest 3.6.0 version. In particular, there are more than 100 available blocks, including filters, transformation, equalization and OFDM blocks.

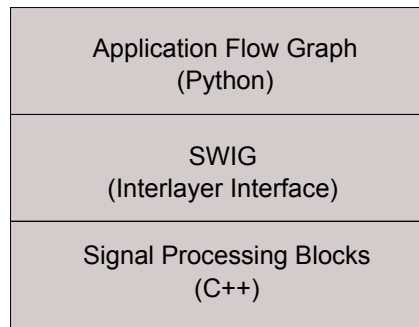


Figure 4.8: GNU Radio-Basic Architecture

C++ implementations. This basic structure is illustrated in Fig. 4.8.

Concisely, GNU Radio provides the necessary environment to realize actual signal processing performed on communication systems. Through the use of this structure, communication protocols, transmission architectures and cross-layer algorithms could be advanced from concept to reality. Especially, the platform is convenient for evaluation purposes of a new design and performance comparisons.

4.7.2 USRP

Besides from signal processing modules, convenient sources to provide inputs to these blocks and modules with monitoring purposes are also required. GNU Radio framework provides several built-in signal source blocks along with the signal sinks, e.g., speakers. Correspondingly, signal sources and sinks have only input and only output ports. In addition to the built-in signal source generators and output monitors, GNU Radio supports another platform, namely USRP, to interact with the real world RF signals.

The main motivation in the design of USRP series is to develop a compatible platform with GNU Radio, providing interactions with real world RF signals. Therefore, conceptually, USRP devices are intended to perform digitization followed by delivery of raw data to the PC when employed on the receive path. On the contrary, reverse processes take place in the transmitter realizations. It should be emphasized that, although being potentially capable of performing signal processing on the hardware, factory default, the most classical configuration, doesn't perform any processing and confers the responsibilities to the computer side. In

this manner, communication with PC is provided over Gigabit ethernet interface.

In general, these devices, manufactured by Ettus Research LLC., are peripherals for implementing software radio applications. The USRP consists of a motherboard, in charge of duplex transformation between analog and digital forms along with interfacing with PC, and a daughterboard bearing the responsibility to implement RF front end. Based on the frequency band of interest and RX/TX capabilities, several daughterboard options are available. Likewise, there exist a few motherboard designs ranging up to the processing potential. In each USRP model, however, basic architecture is built over field programmable gate arrays (FPGA), ADC/DAC pairs and the analog circuitry. Throughout this section, USRP N200 device equipped with RFX2400 daughterboard will be the basis platform for the implementation experiment. In Fig. 4.9, a picture of this hardware platform is shown. Specifically, USRP N200 consists of the combination of main components: Spartan 3A-DSP 1800 FPGA, 100 MS/s dual ADC and 400 MS/s dual DAC. As regards RF front end, RFX2400 takes a part. In addition to the reception capabilities over 2.3-2.9 GHz band, this daughterboard facilitates full duplex transmission between 2.4 and 2.483 GHz. In this sense, this physical combination is a convenient platform to realize ISM band wireless network applications and protocols, such as WiFi and Zigbee.

4.7.3 The Experiment

Based on the foregoing framework and physical hardware, fundamental structure of the proposed scheme has been demonstrated. Before beginning the further details of the implementation, it should be noted that, USRPs are neither supplied from an energy harvester nor have a rechargeable battery. In contrast, these devices are powered by constant AC sources. Consequently, it has not been possible to realize a comprehensive implementation in our testbed. However, by keeping and updating virtual values in registers, battery level and replenished energy inputs are provided by pretending to be supplied by an energy harvesting transmitter. Moreover, the experiment does not have any evaluation purposes and should be regarded as an implementation demonstration.

As stated before, 802.11g standard forms the body structure of the development. As regards the implementation of proposed heuristic, 802.11 specification supports a convenient physical

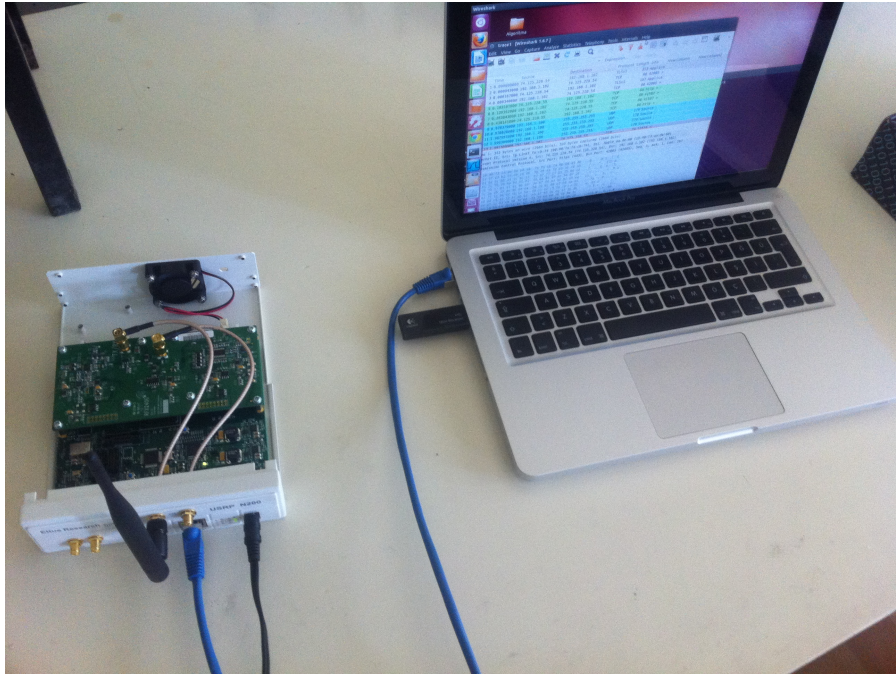


Figure 4.9: Test bed platform used in implementation experiment

rate adaptation infrastructure. Furthermore, the specification has been previously investigated over several SDR platforms [72, 73], and thus is a reasonable starting point. Specifically in [73], authors have presented an implementation of IEEE 802.11 a/g/p transmitter on GNU Radio platform. Although the realization is based on older releases of GNU Radio and physical drivers, fundamental signal processing blocks are still viable. In the rest of the discussion, desired GNU Radio flow graph will be built on these blocks. In short, signal processing operations employed from the study in [73] involve error detection via CRC32, PLCP data frame calculations, scrambling, convolutional encoding, code puncturing, OFDM data interleaving, pilot and cyclic prefix insertions. In addition to these blocks, several built-in processing mechanisms such as symbol mapping, OFDM subcarrier and symbol management have been made use of to complete the design of a fully functional 802.11g transmitter. To this end, convenient MAC header formation and corresponding glueing operations have been realized with respect to the latest GNU Radio release and driver of the physical hardware. Please see Appendix D for further details on implementation and source code adaptation efforts against compatibility issues between older and newer versions of testbed platform.

Based on such a transmission setting, TriMod algorithm is integrated on the top of the struc-

ture. Fundamentally, proposed heuristic checks the length of data queue, channel state and virtual battery to translate the information into a rate decision. Observe that, in order to generate the physical packet to be sent, rate decision should be given beforehand because the rate is an input parameter of packet construction and MAC header formation blocks. Afterwards, MAC header, e.g., source and destination MAC addresses, fragment number etc., is merged into the data packet and corresponding processing blocks format this signal into the final stream. As the details of signal processing operations are out of the scope of this thesis, further details will not be included within this section (Please see [73] for further information).

Contents of data packets are formed according to the real world data traces. Specifically, the traces are created by sniffing the wireless medium⁷ over a network analyzer software called Wireshark [74]. During the course of a regular internet surfing on a PC, another machine is employed to sniff data packets over the air. Sniffing operation is carried on for a few minutes and the transmission from the access point (AP) to the PC is recorded in a file. Ignoring the latency occurred within data buffer of the AP, arrival times and corresponding information bits are saved in an array within the source code and into a text file, respectively. It should be emphasized here that, due to the latency costs of flow graph generation for each data packet and signal processing, the implementation doesn't operate in a real time fashion. In summary, formation process of the stream to the input of the RF front end does take a longer duration than it should be. Therefore, rather than employing timers, variables are used to keep track of the progress. Especially, the variable employed for system operation time is increased as if the intended transmission is completed within a slot. The application checks the available data in the buffer and virtual battery level based on the arrays keeping arrival instants and system operation time variable. Fortunately, overall latency is not within the scale of coherence time and channel state information is still dependable.

Next step is the channel adaptation. In particular, received SNR information is made use of to abstract the CSI. A typical 802.11 receiver is capable of acquiring received signal strength indication (RSSI) during preamble stage. Based on this ability, in addition to the RSSI signal, RSSI noise values could be captured by the receiver. Consequently, at the receiver side, it is possible to derive SNR value in dB by subtracting noise strength from signal strength in dBm.

Finally, the receiver setting shall be clarified. A conventional 802.11g chipset integrated

⁷ Details of the procedure could be found in Appendix D

within the testbed computer is utilized for the monitoring purposes of received frames. In particular, WiFi Link 5100 model wlan adapter by Intel Corporation [75] is the receiver and preferred especially for driver support of monitor mode. Furthermore, by employing the chipset within the testbed computer, feedback channel to obtain channel state is no longer needed. Of course, this is not the case for the target communication settings but meets our need to enhance the demonstration of the proposed scheme. In this sense, corresponding RSSI values are abstracted through the use of Wireshark and recorded periodically in a text file during the operation. In Fig. 4.10, a screenshot captured during the experiment is shown. A more detailed discussion could also be found in Appendix D. Additionally, by formatting the MAC header and frame body in accordance with IEEE 802.11 beacon structure [60], testbed setup is experimented to communicate with other WLAN chips, as well, e.g., chipsets employed within mobile handheld devices.

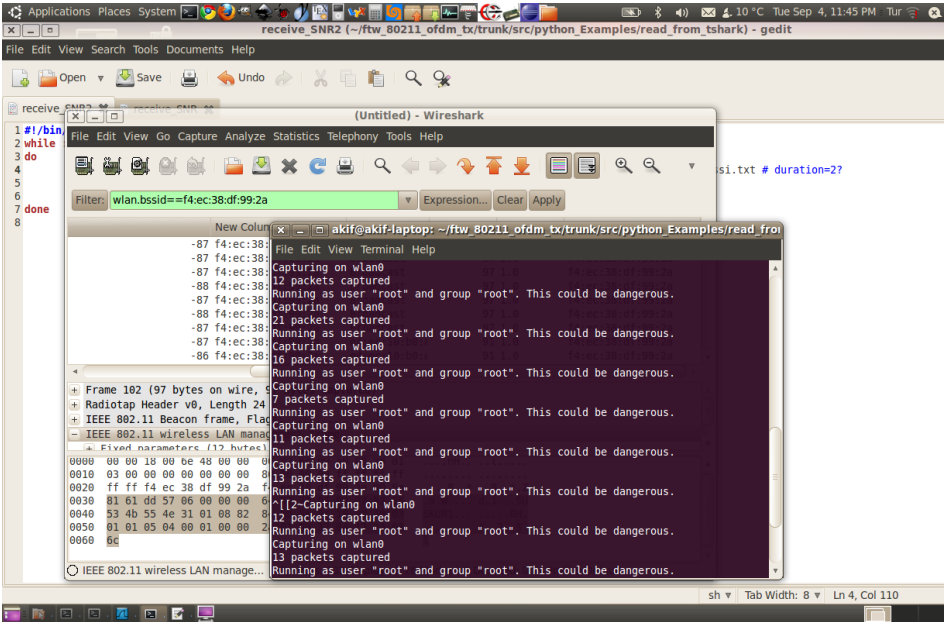


Figure 4.10: A screen view from the experimentation computer

In summary, overall structure described throughout this section implements the fundamental operations of TriMod policy. Although the operation does not fulfil the requirements of a fully functional system due to the lack of hardware configuration and high latency caused by the nature of testbed, the realization demonstrates the practicality of the heuristic.

CHAPTER 5

CONCLUSIONS

This thesis proposes and studies energy-efficient resource allocation techniques for energy scavenging communication systems. Throughout the study, three different transmission rate-power scheduling problems have been taken into account from theoretical and implementation oriented aspects.

Firstly, analysis of two distinct offline formulations, having the ultimate objective of transmission completion time minimization in common, have been considered within Chapter 3. In the first part, structural properties of an optimal allocation under AWGN broadcast channel has been investigated. From a broad perspective, the results have been derived based on the first and second order differential characteristics of the capacity region as a function of average transmit power. Primarily, it has been shown that rate-power allocation stays constant as long as the causality constraints are loose. Along similar lines, it has been established that transmit power course is monotonically increasing and transmit power variations occur due to some certain causality constraints being tight. Second part of the section has been based on a point-to-point communication setting under fading conditions. An iterative solution structure, involving convex optimization methods, is shown to achieve the optimal offline schedule of an energy harvesting transmitter within some ϵ -neighbourhood.

Despite being unrealistic in many scenarios, offline analyses conducted within the first part help us gain a deeper understanding of efficient allocation schemes and obtain upper bounds on the best achievable performance. Although online approaches seem more practical, in general, obtaining an optimal online structure might be intractable. As a matter of fact, because of this issue there has been few theoretical works relaxing the offline assumption. In this manner, offline investigations are extremely worthwhile and, broadly speaking, provide the most valid

benchmarks as in the case considered in numerical examination of the heuristic proposed in this study.

To the best of our knowledge, this thesis bridges the offline and practical investigations for the first time. Specially in the second half of the study, intuitions derived from optimal offline structures were pointed out regarding implementability and physical concerns. First, discrete nature of achievable transmit power and rate set has been emphasized. Afterwards, we have stated the issues regarding power amplifiers and channel interpretation. Comparing the two main classes of channel estimation, challenges within each have been stated. Additionally, correlation between the allocation scheme, hardware and cross-layer design requirements have been pointed out along with the suggestions regarding design process. Based on these observations, an implementable scheduling scheme TriMod was developed. For the evaluation purpose of TriMod, a widespread transmission specification having concave increasing characteristics of energy per bit as a function of rate, IEEE 802.11, was employed. Beginning with the long-term examinations over a well-known 802.11 rate adaptation scheme, structure of the proposal has been compared to the offline optimal in a few short run. It has been concluded about these investigations that, TriMod bears strong resemblances to optimal offline solution by means of structural properties and outperforms conventional 802.11 adaptation schemes for the setting of interest. Especially, numerical experiments conducted within Chapter 4 show the urgent need to develop rechargeable transmitter-specific transmission mechanisms.

Finally, a demonstration of practicality experiment has been realized by implementing the fundamental allocation architecture on a certain development platform. In particular, based onto the software radio implementation of IEEE 802.11 a/g/p by a previous study, proposed scheme is integrated within the design. Explaining the details of the experimentation to keep continuity of the research, we have come to the conclusion that the policy has significant implementation potential and could be employed within appropriate architectures.

Energy scavenging technologies enables promising advances within a wide range of telecommunication applications. The ability to operate independent of a constant power source is an important design goal and provides desirable flexibilities, enabling even new markets and application fields. Due to rising smart phone market and the trend in the interaction of these devices with the physical world, for instance, rechargeable WLAN devices could be employed

within public places to inform visitors about the location or even facilitate services like *pay by phone*. To this end, however, much more work should be done including the further advancement of harvesting technologies and design of novel practical schemes. As regards future direction of this study, a few issues that have yet to be pursued are summarized below.

Firstly, consideration of the offline analysis could be extended to the network problems. Investigating the scheduling structure along with the MAC and network layer schemes, might provide insights and inspire the design of practical algorithms. In fact, as compared to the online studies, there has been a few offline investigations so far. Especially by means of mathematical approaches, future efforts should also be concentrated on the development of online solutions to gain better understanding.

As previously stated, theoretical studies should be combined with the practicality considerations to produce implementable smart schedules. This research takes such a responsibility and progresses in this direction. Likewise, other analytical investigations in the literature should be carried onto the more realistic scenarios and practicality. Due to the hardware limitations of the experiment setup, however, a fully functional implementation has not been possible.

A more reasonable testbed, however, can be developed by combining off-the-shelf transmitter subunits, such as transmitter module, processor, harvester and a rechargeable battery. As an example, a WLAN transmitter module with transmission power and rate adaptation capabilities could be equipped with an ARM processor, a solar harvester, a NiMH battery and a battery monitoring IC. Likewise, similar designs could be developed for the employment and performance evaluation of TriMod scheme. In the view of the author, design of a convenient standalone rechargeable transmitter along with the realization of the proposed scheme should be the further direction of this work.

REFERENCES

- [1] International Energy Agency, “Energy Technology Scenarios and Strategies For a More Secure and Sustainable Energy Future,” Paris, June 2006.
- [2] A. Kansal, J. Hsu, S. Zahedi and M. B. Srivastava, “Power management in energy harvesting sensor networks,” *ACM. Trans. Embedded Computing Systems*, May. 2006.
- [3] C. Vigorito, D. Ganesan, , and A. Barto. “Adaptive control of duty-cycling in energy-harvesting wireless sensor networks,” In *Proc. IEEE SECON*, San Diego, CA, 2007.
- [4] V. Sharma, U. Mukherji, V. Joseph, and S. Gupta, “Optimal energy management policies for energy harvesting sensor nodes,” *IEEE Trans. on Wireless Communications*, 9(4):1326-1336, April 2010.
- [5] K. Lin, J. Hsu, S. Zahedi, D. Lee, J. Friedman, A. Kansal, V. Raghunathan, M. Srivastava, “Heliomote: Enabling long-lived sensor networks through solar energy harvesting,” in *Proceedings of the 3rd International Conference on Embedded Networked Sensor Systems (SenSys)*, San Diego, CA, USA, p. 309, 2005.
- [6] H. Erkal, *Optimization Of Energy Harvesting Wireless Communication Systems*, M.Sc. Thesis, Middle East Technical University, Dept. of Electrical and Electronics Engineering, Ankara, Turkey, Dec. 2011.
- [7] O. Ozel, K. Tutuncuoglu, J. Yang, S. Ulukus and A. Yener, “ Transmission with Energy Harvesting Nodes in Fading Wireless Channels: Optimal Policies,” *IEEE Jour. on Selected Areas in Communications*, 29(8):1732-1743, Sept. 2011.
- [8] J. He, P. Loskot, T. O’Farrell *et al.*, “Energy efficient architectures and techniques for Green Radio access networks,” *IEEE CHINACOM*, Aug. 2010.
- [9] C. Han *et al.*, “Green radio: radio techniques to enable energy-efficient wireless networks,” *IEEE Communications Magazine*, 49(6), pp. 46-54, June 2011.
- [10] T. Chen, Y. Yang, H. Zhang, H. Kim, and K. Horneman, “Network energy saving technologies for green wireless access networks,” *IEEE Wireless Communications*, vol. 18, no. 5, pp. 30-38, Oct. 2011.
- [11] W. Ye, J. Heidemann, D. Estrin, “An energy-efficient MAC protocol for wireless sensor networks,” *IEEE INFOCOM*, California, June 2002.
- [12] R. C. Shah, J. M. Rabaey, “Energy aware routing for low energy ad hoc sensor networks,” *IEEE WCNC*, California, March 2002.
- [13] O. Ozel and S. Ulukus, “Information-Theoretic Analysis of an Energy Harvesting Communication System,” in *IEEE PIMRC Workshops*, 2010.

- [14] R. Rajesh, V. Sharma, and P. Viswanath, "Information Capacity of Energy Harvesting Sensor Nodes," *2011 IEEE Int. Symposium on Information Theory*, St.Petersburg, Aug. 2011.
- [15] R. Rajesh, V. Sharma and P. Viswanath, "Capacity of Fading Gaussian Channel with an Energy Harvesting Sensor Node," in *IEEE GLOBECOM'11*, Texas, Dec. 2011.
- [16] V. Sharma, R. Rajesh, "Queuing Theoretic and Information Theoretic Capacity of Energy Harvesting Sensor Nodes," *Asilomar Conference on Signals, Systems, and Computers*, Monterey, CA, Nov. 2011.
- [17] R. Rajesh, P. K. Deekshith and V. Sharma, "Capacity of Gaussian MAC Powered by Energy Harvesters without Storage Buffer," arXiv:1204.4905v1, April 2012.
- [18] R. Vaze, "Transmission Capacity of Wireless Ad Hoc Networks with Energy Harvesting Nodes," arXiv:1205.5649v1, May 2012.
- [19] C. Moser, L. Thiele, D. Brunelli, L. Benini, "Adaptive Power Management in Energy Harvesting Systems," *DATE'07: Proceedings of the conference on design, automation and test in Europe*, NY, pp. 773-778, ACM Press, 2007.
- [20] E. Uysal-Biyikoglu, B. Prabhakar, and A. El Gamal, "Energy-efficient Packet Transmission over a Wireless Link," *IEEE Transactions on Networking*, vol.10, pp.487-499, Aug. 2002.
- [21] E. Uysal-Biyikoglu and A. El Gamal, "Energy-efficient Packet Transmission Over a Multi-access Channel," *Proc. IEEE Intl. Symposium on Information Theory*, p.153, July 2002.
- [22] R. A. Berry and R. G. Gallager, "Communication over fading channels with delay constraints," *IEEE Transactions on Information Theory*, vol.48, pp.1135-1149, May 2002.
- [23] P. Nuggehalli, V. Srinivashan, and R. R. Rao, "Delay constrained energy efficient transmission strategies for wireless devices," *Proc. IEEE INFOCOM*, vol.3, pp.1765-1772, New York, June 2002.
- [24] M. A. Zafer and E. Modiano, "A calculus approach to energy-efficient data transmission with quality of service constraints," *IEEE Transactions on Networking*, vol.17, pp.898-911, June 2009.
- [25] J. Yang and S. Ulukus, "Optimal Packet Scheduling in an Energy Harvesting Communication System," *IEEE Trans. on Communications*, 60(1):220-230, January 2012.
- [26] K. Tutuncuoglu and A. Yener, "Optimum Transmission Policies for Battery Limited Energy Harvesting Nodes," *IEEE Trans. on Wireless Communications*, 11(3):1180-1189, March 2012.
- [27] D. Gunduz, "Energy Harvesting Communication System with Battery Constraint and Leakage," *IEEE GLOBECOM'11*, Texas, Dec. 2011.
- [28] M. A. Anteppli, E. Uysal-Biyikoglu, and H. Erkal, "Optimal Packet Scheduling on an Energy Harvesting Broadcast Link," to appear on *IEEE Journal on Selected Areas in Communications (JSAC), Special Issue on Energy-Efficient Wireless Communications*, 2011.

- [29] J. Yang, O. Ozel and S. Ulukus, "Broadcasting with an Energy Harvesting Rechargeable Transmitter," *IEEE Transactions on Wireless Communications*, vol.11, pp.571-583, February 2012.
- [30] O. Ozel, J. Yang and S. Ulukus, "Broadcasting with a Battery Limited Energy Harvesting Rechargeable Transmitter," *International Symposium on Modeling and Optimization in Mobile, Ad Hoc and Wireless Networks (WiOpt)*, pp.205-212, Princeton, NJ, May 2011.
- [31] O. Ozel, J. Yang and S. Ulukus, "Optimal Transmission Schemes for Parallel and Fading Gaussian Broadcast Channels with an Energy Harvesting Rechargeable Transmitter," *Elsevier Computer Communications*, to appear.
- [32] Y. Luo, J. Zhang, K. B. Letaief, "Training Optimization for Energy Harvesting Communication Systems," arXiv:1207.2608v2, July 2012.
- [33] D. Gunduz and B. Devillers, "Two-hop communication with energy harvesting," *Proc. CAMSAP*, San Juan, Dec. 2011.
- [34] O. Orhan, E. Erkip, "Energy Harvesting Two-hop Networks: Optimal Policies for the Multi-Energy Arrival Case," *IEEE SARNOFF*, New Jersey, May 2012.
- [35] C. Huang, R. Zhang, S. Cui, "Throughput Maximization for the Gaussian Relay Channel with Energy Harvesting Constraints," arXiv:1109.0724v2, May 2012.
- [36] N. Tekbiyik, T. Girici, E. Uysal-Biyikoglu, and K. Leblebicioglu "Proportional Fair Resource Allocation on an Energy Harvesting Downlink - Part I: Structure," arXiv:1205.5147v1, May 2012.
- [37] N. Tekbiyik, T. Girici, E. Uysal-Biyikoglu, and K. Leblebicioglu "Proportional Fair Resource Allocation on an Energy Harvesting Downlink - Part II: Algorithms," arXiv:1205.5153v1, May 2012.
- [38] F. Simjee and P. H. Chou, "Everlast: Long-life, Supercapacitor-operated Wireless Sensor Node," *Proc. International Symposium on Low Power Electronics and Design*, pp. 197-202, 2006.
- [39] M. Barnes, C. Conway, J. Mathews and D. K. Arvind, "ENS: An Energy Harvesting Wireless Sensor Network Platform," *International Conference on Systems and Networks Communications*, Nice, France, Aug 2010.
- [40] J. A. Paradiso and M. Feldmeier, "A Compact, Wireless, Self-Powered Push button Controller," *Proc. 3rd International Conference on Ubiquitous Computing* pp. 299-304, 2001.
- [41] N. Shenck and J. Paradiso, "Energy Scavenging with Shoe-mounted Piezoelectrics," *IEEE Micro*, 21(3), pp. 30-42, June 2001.
- [42] C. Park and P. Chou, "AmbiMax: Autonomous Energy Harvesting Platform for Multi-Supply Wireless Sensor Nodes," *3rd Annual IEEE Communications Society on Sensor and Ad Hoc Communications and Networks*, vol. 1, pp. 168-177, Sept. 2006.
- [43] M. Weimer, T. Paing, and R. Zane, "Remote Area Wind Energy Harvesting for Low-power Autonomous Sensors," *IEEE Power Electronics Specialists Conference*, pp. 1-5, June 2006.

- [44] M. Buettner, B. Greenstein, A. Sample, J. R. Smith, and D. Wetherall, "Revisiting Smart Dust with RFID Sensor Networks," *Proc. ACM Workshop on Hot Topics in Networks (Hotnets-VII)*, Oct.2008.
- [45] A. P. Sample, D. J. Yeager, P. S. Powledge, A. V. Mamishev, and J. R. Smith, "Design of an RFID-Based Battery-Free Programmable Sensing Platform," *IEEE Trans. Instrum. Meas.* ,57(11), pp. 2608-2615, 2008.
- [46] *GT-S7550 User-Manual*, Samsung Electronics.
- [47] S. Chen, P. Sinha, N. B. Shroff and C. Joo, "Finite-Horizon Energy Allocation and Routing Scheme in Rechargeable Sensor Networks," *IEEE INFOCOM*, Shanghai, China, April 2011.
- [48] M. Gatzianas, L. Georgiadis and L. Tassiulas, "Control of Wireless Networks with Rechargeable Batteries," *Trans. on Wireless Communications*, vol.9, pp.581-593, Feb. 2010.
- [49] S. Boyd and L. Vandenberghe, *Convex Optimization*, Cambridge University Press, 2004.
- [50] D. G. Luenberger, *Linear and Nonlinear Programming*, Springer, 2008.
- [51] P.A.Jensen and J.F. Bard, *Algorithms for Constrained Optimization*, 2003, available at http://www.me.utexas.edu/~jensen/ORMM/supplements/units/nlp_methods/const_opt.pdf, last accessed on Sept. 2012.
- [52] S. Shakkottai, T. Rappaport, and P. Karlsson, "Cross-layer design for wireless networks," *IEEE Communications Magazine*, 41(10), pp. 74-80, Oct 2003.
- [53] K. Mandke, R. C. Daniels, S.-H. Choi, S. M. Nettles, and R. W. Heath, Jr., "Physical Concerns for Cross-Layer Prototyping and Wireless Network Experimentation," *Proc. of the Second WiNTECH*, Sep. 2007.
- [54] J. Camp and E. Knightly, "Modulation Rate Adaptation in Urban and Vehicular Environments: Cross-Layer Implementation and Experimental Evaluation," *IEEE Transactions on Networking*, 18(6), pp. 1949-1962, Dec. 2010.
- [55] M. Vutukuru, H. Balakrishnan, and K. Jamieson, "Cross-layer wireless bit rate adaptation," *Proc. ACM SIGCOMM*, Barcelona, Spain, Aug. 2009.
- [56] A. J. Goldsmith and S. G. Chua, "Variable-rate variable-power MQAM for fading channels," *IEEE Transactions on Communications*, vol. 45, pp. 1218-1230, Oct. 1997.
- [57] V. Raghunathan, A. Kansal, J. Hsu, J. Friedman, and M. Srivastava. "Design consideration for solar energy harvesting wireless embedded systems," *IEEE IPSN*, California, April 2005.
- [58] J. Taneja, J. Jeong, and D. E. Culler. "Design, modeling, and capacity planning for micro-solar power sensor networks," *IEEE IPSN*, Missouri, April 2008.
- [59] A. J. Goldsmith, *Wireless Communications*. Cambridge University Press, 2005.
- [60] IEEE LAN/MAN Committee, "Wireless LAN Medium Access Control (MAC) and Physical Layer (PHY) Specifications," *IEEE*, 2003.

- [61] A. Kamerman and L. Monteban, "WaveLAN-II: A High-performance wireless LAN for the unlicensed band. *Bell Labs Technical Journal*, pp. 118-133, Summer 1997.
- [62] J. P. Pavon and S. Choi, "Link adaptation strategy for IEEE 802.11 WLAN via received signal strength measurement," *IEEE ICC*, volume 2, pp. 1108-1113, Alaska, May 2003.
- [63] D. Qiao, S. Choi, A. Jain, and K. G. Shin, "MiSer: An Optimal Low-energy Transmission Strategy for IEEE 802.11a/h. *ACM MOBICOM*, pp. 161-175, California, September 2003.
- [64] M. Lacage, M. H. Manshaei, and T. Turetli. "IEEE 802.11 Rate Adaptation: A Practical Approach," *ACM MSWiM*, 2004.
- [65] J. Bicket. *Bit-rate selection in wireless networks*, M.Sc. Thesis, Massachusetts Institute of Technology, Dept. of Electrical Engineering and Computer Science, February 2005.
- [66] W. Kim, M. O. Khan, K. T. Truong, S-H. Choi, R. Grant, H. Wright, K. Mandke, R. C. Daniels, R. W. Heath, Jr., and S. Nettles, "An Experimental Evaluation of Rate Adaptation for Multi-Antenna Systems," *IEEE INFOCOM*, Rio de Janeiro, Apr. 2009.
- [67] C. Heegard, "Range versus rate in IEEE 802.11g wireless local area networks," presented in September meeting IEEE 802.11 Task Group G, Sept. 2001, available at <http://www.nativei.com/heegard/papers/RvR.pdf>, last accessed on Sept. 2012.
- [68] M. Dillinger, K. Madani, N. Alonistioti, *Software Defined Radio Architectures, Systems and Functions*, Wiley, 2003.
- [69] J. Mitola and G. Q. Maguire, "Cognitive radios: Making software radios more personal," *IEEE Personal Communications*, vol. 6, pp. 13-18, Aug. 1999.
- [70] Official GNU software radio website. <http://gnuradio.org>, last accessed on Sept. 2012.
- [71] Ettus Research LLC website. <http://www.ettus.com>, last accessed on Sept. 2012..
- [72] K. Mandke, S. Choi, G. Kim, R. Grant, R. C. Daniels, W. Kim, R. W. Heath, Jr., and S. Nettles, "Early Results on Hydra: A Flexible MAC/PHY Multihop Testbed," *IEEE VTC*, Dublin, Ireland, Apr. 2007.
- [73] P. Fuxjager, A. Costantini, D. Valerio, P. Castiglione, G. Zacheo, T. Zemen, F. Ricciato "IEEE 802.11p Transmission Using GNURadio," *6th Karlsruhe Workshop On Software Radios*, Karlsruhe, Germany, March 2010.
- [74] Official Wireshark website. <http://www.wireshark.org>, last accessed on Sept. 2012..
- [75] Intel WiFi Link 5100 product brief, available at <http://www.intel.com/content/dam/www/public/us/en/documents/product-briefs/wifi-link-5100-brief.pdf>, last accessed on Sept. 2012..
- [76] Source codes of the experimentation, available at <http://www.eee.metu.edu.tr/~cng>, last accessed on Sept. 2012.

Appendix A

PROOF OF LEMMA 3.1.2

The claim is that power is non-decreasing with epoch number i . Equivalently (cf. Lemma 3.1.1) power is non-decreasing in time. To show this, we will argue that given a schedule during which power decreases at some time t_i , this schedule can only be improved by equating the power levels before and after t_i . Consider a time interval (τ_1, τ_2) , so that power is constant at $P_1 > 0$ during (τ_1, t_i) , and at $P_2 < P_1$ during (t_i, τ_2) . As illustrated in Fig A.1, let $t = \tau_2 - \tau_1$, and the lengths of the constant-power slots be βt and $(1 - \beta)t$. Denote the rate pairs in the 1st and 2nd slots as (r_{11}, r_{21}) and (r_{12}, r_{22}) , respectively. We will show that keeping the total

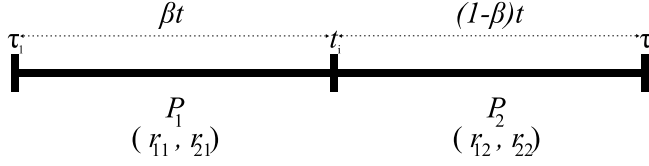


Figure A.1: Illustration of the transmission scheme used in Lemma 3.1.2.

consumed energy constant, and transferring some amount of energy ΔE from the first slot to the second such that power levels are reallocated closer together, the sender can transmit at least the same number of bits within the same duration. Let us denote the average rate of the 2nd user as $\bar{r}_2 \triangleq \beta r_{21} + (1 - \beta)r_{22}$. Provided $r_{21} > 0$, the sender could transfer some energy and some of user 2's bits from the first epoch to the second while keeping user 1's rates r_{11} and r_{12} constant. As energy and bits are simply being deferred for later use, this operation does not violate feasibility. Specifically, let

$$P'_1 = P_1 - (1 - \beta)\Delta P, P'_2 = P_2 + \beta\Delta P. \quad (\text{A.1})$$

such that the new power allocation to the slots is (P'_1, P'_2) satisfying $P_2 \leq P'_2 \leq P'_1 \leq P_1$. With this new allocation, the 2nd user's rate in the first slot is $h_2(P'_1, r_{11}) \leq h_2(P_1, r_{11}) = r_{21} > 0$.

Its new new average rate over the duration of t is:

$$\begin{aligned}
\bar{r}_2 &= h_2(P'_1, r_{11})\beta + h_2(P'_2, r_{12})(1 - \beta) \\
&\geq h_2(P_1, r_{11})\beta + h_2(P_2, r_{12})(1 - \beta) \\
&= \bar{r}_2
\end{aligned} \tag{A.2}$$

This is shown by straightforward application of the properties listed in section 3.2.1

(A.2) follows from the fact that

$$\begin{aligned}
&h_2(P'_1, r_{11})\beta + h_2(P'_2, r_{12})(1 - \beta) \\
&- h_2(P_1, r_{11})\beta - h_2(P_2, r_{12})(1 - \beta) \geq 0
\end{aligned} \tag{A.3}$$

for all $\beta = \{0, 1\}$ with equality achieved at $\beta = 0, 1$.

$$\begin{aligned}
f(\beta) &= h_2(P_1 - (1 - \beta)\Delta P, r_{11})\beta \\
&\quad + h_2(P_2 + \beta\Delta P, r_{12})(1 - \beta) \\
&\quad - h_2(P_1, r_{11})\beta - h_2(P_2, r_{12})(1 - \beta)
\end{aligned} \tag{A.4}$$

The concavity of $f(\beta)$ in β implies that (A.3) holds.

The 1st and 2nd order derivatives of f with respect to β are the following¹

$$\begin{aligned}
\frac{\partial f}{\partial \beta} &= h_2(P_1 - (1 - \beta)\Delta P, r_{11}) - h_2(P_2 + \beta\Delta P, r_{12}) \\
&\quad + \beta \{h_{2_x}(P_1 - (1 - \beta)\Delta P, r_{11})(\Delta P)\} \\
&\quad + (1 - \beta) \{h_{2_x}(P_2 + \beta\Delta P, r_{12})(\Delta P)\} \\
&\quad - h_2(P_1, r_{11}) + h_2(P_2, r_{12})
\end{aligned} \tag{A.5}$$

$$\begin{aligned}
\frac{\partial^2 f}{\partial \beta^2} &= 2 \underbrace{(h_{2_x}(P_1 - (1 - \beta)\Delta P, r_{11})(\Delta P) - h_{2_x}(P_2 + \beta\Delta P, r_{12})(\Delta P))}_{\leq 0} \\
&\quad + \beta \left\{ \underbrace{h_{2_{xx}}(P_1 - (1 - \beta)\Delta P, r_{11})(\Delta P)^2}_{\leq 0} \right\} \\
&\quad + (1 - \beta) \left\{ \underbrace{h_{2_{xx}}(P_2 + \beta\Delta P, r_{12})(\Delta P)^2}_{\leq 0} \right\} \\
&\leq 0
\end{aligned} \tag{A.6}$$

¹ h_{2_x} and $h_{2_{xx}}$ represent the first and second order partial derivatives of h_2 with respect to P , respectively.

According to assumptions (1-5) about rate functions given in Section 3.2.1, (A.6) always holds.

In the remaining case which is $r_{21} = 0$, we know that $r_{11} > 0$ must hold (as $P_1 > 0$.) In this case, the allocation can similarly be improved by bringing power levels closer and transferring some of the first user's bits to the right, while keeping the rate allocation of the 2^{nd} user unchanged. Let $\bar{r}_1 \triangleq \beta r_{11} + (1 - \beta)r_{12}$ be the average rate over the duration t of the 1^{st} user. After the reallocation, the average rate of the 1^{st} user becomes

$$\begin{aligned}\bar{r}_1 &= h_1(P'_1, r_{21})\beta + h_1(P'_2, r_{22})(1 - \beta) \\ &\geq h_1(P_1, r_{21})\beta + h_1(P_2, r_{22})(1 - \beta) \\ &= \bar{r}_1\end{aligned}\tag{A.7}$$

(A.7) follows from the fact that

$$\begin{aligned}h_1(P'_1, r_{21})\beta + h_1(P'_2, r_{22})(1 - \beta) \\ - h_1(P_1, r_{21})\beta - h_1(P_2, r_{22})(1 - \beta) \geq 0\end{aligned}\tag{A.8}$$

for all $\beta = \{0, 1\}$ with equality achieved at $\beta = 0, 1$.

$$\begin{aligned}q(\beta) &= h_1(P_1 - (1 - \beta)\Delta P, r_{21})\beta + h_1(P_2 + \beta\Delta P, r_{22})(1 - \beta) \\ &\quad - h_1(P_1, r_{21})\beta - h_1(P_2, r_{22})(1 - \beta).\end{aligned}\tag{A.9}$$

We can show that (A.8) holds by proving $q(\beta)$ is concave in β .

The 1^{st} and 2^{nd} order derivatives of q with respect to β are the following²

$$\begin{aligned}\frac{\partial q}{\partial \beta} &= h_1(P_1 - (1 - \beta)\Delta P, r_{21}) + \beta \{h_{1,x}(P_1 - (1 - \beta)\Delta P, r_{21})(\Delta P)\} \\ &\quad - h_1(P_2 + \beta\Delta P, r_{22}) + (1 - \beta) \{h_{1,x}(P_2 + \beta\Delta P, r_{22})(\Delta P)\} \\ &\quad - h_1(P_1, r_{21}) + h_2(P_2, r_{22})\end{aligned}\tag{A.10}$$

² $h_{1,x}$ and $h_{1,xx}$ represent the first and second order partial derivatives of h_1 with respect to P , respectively.

$$\begin{aligned}
\frac{\partial^2 q}{\partial \beta^2} &= 2 \underbrace{(h_{1,x}(P_1 - (1 - \beta)\Delta P, r_{21})(\Delta P) - h_{1,x}(P_2 + \beta\Delta P, r_{22})(\Delta P))}_{\leq 0} \\
&\quad + \beta \left\{ \underbrace{h_{1,xx}(P_1 - (1 - \beta)\Delta P, r_{21})(\Delta P)^2}_{\leq 0} \right\} \\
&\quad + (1 - \beta) \left\{ \underbrace{h_{1,xx}(P_2 + \beta\Delta P, r_{22})(\Delta P)^2}_{\leq 0} \right\} \\
&\leq 0
\end{aligned} \tag{A.11}$$

According to the properties listed in section 3.2.1, (A.11) always holds if $r_{21} \geq r_{22}$. Hence q is concave in β , if $r_{21} = 0$.

We conclude that a policy that contains a drop in power level is sub-optimal. ■

Appendix B

PROOF OF LEMMA 3.1.3

To reach contradiction, suppose that power increases at time t_i ($P_{i+1} > P_i$). We will show that if none of the conditions (a), (b) or (c) hold, then it is possible to improve the schedule by transferring some energy from the $(i + 1)^{th}$ epoch to the i^{th} . Assuming the i^{th} epoch length is βt and the $(i + 1)^{th}$ is $(1 - \beta)t$, after bringing power levels closer, we obtain:

$$P'_i = P_i + \beta\Delta P, P'_{i+1} = P_{i+1} - (1 - \beta)\Delta P. \quad (\text{B.1})$$

Observe that if we treat P_i as P_2 and P_{i+1} as P_1 , then (B.1) becomes identical with (A.1). This implies that at least the same number of bits could be transmitted to 2^{nd} user, if we can bring power levels closer while keeping the 1^{st} user's rates constant. In addition to this, the allocation could also be improved by bringing power levels while keeping the 2^{nd} user's rates constant, in case $r_{2i-1} \geq r_{2i}$. Consequently, equations (A.2) and (A.7) hold.

It is straightforward that we cannot bring power levels any closer when condition (a) holds, due to the energy causality constraint. Secondly, it also doesn't yield a better schedule, if we can not transfer data from the latter epoch to the former(condition (b)). When it is possible to transfer some positive amount of energy from the $(i + 1)^{th}$ epoch to the i^{th} , as shown in (A.2), we can always improve allocation while keeping the rates of the 1^{st} user the same. Although bringing power levels closer while keeping the rates of the 1^{st} user the same is not feasible in case 2^{nd} user's bit constraint is active, we may still improve allocation as proved in (A.7). Nevertheless, this time we require $r_{2i-1} \geq r_{2i}$. As rate of the 2^{nd} user can only rise upon a data arrival for the 2^{nd} user, in case 2^{nd} user's bit constraint is active, condition (c) describes the last case that we may not improve allocation by bringing power levels closer. We have thus shown that this set of three conditions contains all the cases in which power can rise, if none of these hold, then power cannot rise. It is straightforward to show that this set cannot be further reduced, by finding counterexamples for each one of conditions (a), (b) and (c).

Appendix C

PROOF OF LEMMA 3.2.1

Consider two feasible allocation vectors \mathbf{r}^A and \mathbf{r}^B and let \mathbf{r}^* be a linear combination of these. We will show that rate allocation vector $\mathbf{r}^* = \theta\mathbf{r}^A + (1 - \theta)\mathbf{r}^B$ is also feasible and consumes an amount of energy less than $\theta E^A(T) + (1 - \theta)E^B(T)$. First, let us compute the energy consumption of \mathbf{r}^* .

$$\begin{aligned} E^*(T) &= \sum_{i=1}^{k^*} g(r_i^*)\xi_i + g(r_{k^*+1}^*)(T - \sum_{i=1}^{k^*} \xi_i) \\ &= \sum_{i=1}^{k^*} g(\theta r_i^A + (1 - \theta)r_i^B)\xi_i \end{aligned} \tag{C.1}$$

$$\begin{aligned} &+ (\theta r_{k^*+1}^A + (1 - \theta)r_{k^*+1}^B)(T - \sum_{i=1}^{k^*} \xi_i) \\ &\leq \sum_{i=1}^{k^*} (\theta g(r_i^A) + (1 - \theta)g(r_i^B))\xi_i \\ &+ (\theta g(r_{k^*+1}^A) + (1 - \theta)g(r_{k^*+1}^B))(T - \sum_{i=1}^{k^*} \xi_i) \tag{C.2} \\ &= \theta E^A(T) + (1 - \theta)E^B(T) \end{aligned}$$

(C.2) follows from the strict convexity of $g(r)$ function and equality holds only if $r^A = r^B$ or $\theta \in \{0, 1\}$. With this inequality, \mathbf{r}^* allocation consumes less than $\theta E^A(T) + (1 - \theta)E^B(T)$. We are now ready to check feasibility of the allocation and begin with the energy causality constraint, (3.10).

$$\begin{aligned} \sum_{i=1}^k g(r_i^*)\xi_i &= \sum_{i=1}^k g(\theta r_i^A + (1 - \theta)r_i^B)\xi_i \\ &\leq \theta \sum_{i=1}^k g(r_i^A)\xi_i + (1 - \theta) \sum_{i=1}^k g(r_i^B)\xi_i \\ &\leq \theta E(t_k) + (1 - \theta)E(t_k) = E(t_k) \end{aligned} \tag{C.3}$$

(C.3) states the satisfaction of energy causality constraint. Similarly, \mathbf{r}^* also respects data causality, (3.11).

$$\begin{aligned} \min\left\{\sum_{i=1}^k r_i^A \xi_i, \sum_{i=1}^k r_i^B \xi_i\right\} &\leq \sum_{i=1}^k (\theta r_i^A + (1-\theta)r_i^B)\xi_i \\ &\leq \max\left\{\sum_{i=1}^k r_i^A \xi_i, \sum_{i=1}^k r_i^B \xi_i\right\} \end{aligned} \quad (\text{C.4})$$

As \mathbf{r}^A and \mathbf{r}^B are two feasible schedules, (C.4) implies that \mathbf{r}^* satisfies data causality constraint. In addition, we have the following when the transmission ends:

$$\begin{aligned} &\sum_{i=1}^{k^*} r_i^* \xi_i + r_{k^*+1}(T - \sum_{i=1}^{k^*} \xi_i) \\ &= \theta \sum_{i=1}^{k^*} r_i^A \xi_i + (1-\theta) \sum_{i=1}^{k^*} r_i^B \xi_i \\ &\quad + \theta r_{k^*+1}^A (T - \sum_{i=1}^{k^*} \xi_i) + (1-\theta) r_{k^*+1}^B (T - \sum_{i=1}^{k^*} \xi_i) \\ &= \theta B(T) + (1-\theta)B(T) = B(T) \end{aligned} \quad (\text{C.5})$$

(C.5) shows the satisfaction of (3.12). So, we have shown that feasible allocations form a convex region, i.e., any linear combination of two feasible schedules is also feasible. Combining this result with (C.2), we conclude that problem 3 is a convex optimization problem.

■

Appendix D

IMPLEMENTATION DETAILS

Complete experimentation setup is given in Table D.1. As noted below, all the experimentations have been built on a Linux-based operating system (OS), Ubuntu. Along with Fedora, this distribution is reported to be the most compatible operating system with GNU Radio (As will be clarified later, there are other reasons to prefer a Linux-based OS). Building and installation process of GNU Radio on Ubuntu Linux is quite easy and instructions given in [70] could be followed. Especially, *build-gnuradio* script is recommended for the beginners.

Table D.1: Test-equipment details

Distribution	Ubuntu 10.04 (32-bit version)
Kernel version	2.6.32-33-generic
GNURadio Version	3.6.0
Python Version	2.7.3
USRP N200 HW revision	rev4
Daughterboard model	RFX2400

After the completion of GNU Radio installation steps, USRP devices could be interfaced with the computer. Firstly, note that, the computer should be equipped with a gigabit ethernet adapter to communicate with the hardware. Even though it is possible to interface the computer through a gigabit ethernet switch, it is highly recommended to experiment on a computer with gigabit ethernet support. Additionally, a first time user will most probably be required to update firmware release of USRP hardware since the factory default firmwares are generally not up-to-date. For this purpose, instructions given in [71] might be followed.

All the referred codes used during the experimentation could be found in [76]. As stated earlier in Chapter 4, overall structure is developed onto the 802.11 a/g/p implementation in [73]. As the foregoing realization was based on an older release, some compatibility issues have

been faced. Firstly, USRP sink arrangement is reconfigured with respect to the updates in GNU Radio. In comparison to the older releases, sink configuration has been simplified and now it is possible to configure the sink by just stating the ADC port and channel number along with the sampling rate. In this manner, sampling rate is set to 20 MHz in accordance with the 802.11g specifications. In addition, due to the structural changes in GNU Radio source tree, some of the signal processing blocks have been imported from the appropriate modules and attributes of these blocks are updated accordingly. Likewise, another issue to be handled was to modify the flow graph so that multi packet transmission could be supported. As a matter of fact, the original implementation supports more than one packet transmission within a run. However, all the packets consist of the same message and the content cannot be changed during the transmission course. Therefore, design of the flow graph has been adapted so that transmission of packets with different information and sizes could be realized. For a deeper understanding, source codes in [76] could be examined.

In the receiver side, Wireshark is utilized to display the received messages. To this end, however, WLAN chipset is required to be operating in monitor mode. In fact, sniffing the wireless medium within monitor mode is not supported by all chipsets. Even though the hardware is capable of operation, a convenient driver with monitor mode support is required. In commercial OS platforms like Windows, drivers are closed-source and, in general, distributions by vendors don't support sniffing. In contrast, it is possible to find convenient drivers supplying monitor mode functionality in Linux-based platforms. Before beginning the sniffing operation, corresponding configurations to operate in monitor mode is necessary because in the default case, wireless cards mostly operate under managed mode, relying on an access point to connect to the network. Although configuration steps may vary based on the driver and vendor, following commands work in most cases:

```
sudo ifconfig wlan0 down
sudo iwconfig wlan0 mode monitor
sudo iwconfig wlan0 channel <channel.number>
sudo ifconfig wlan0 up
```

Indeed, the third command given above is not a part of monitor mode configuration process. However, it is necessary to capture the desired packets. In IEEE 802.11g standard, there are 14 possible channels to be used, with center frequencies of sequential channels separated by 5 MHz. First 13 of these channels are supported in Europe. Unless the appropriate channel over which transmitter operates is specified, reception is not likely to occur.

As the final point, channel interpretation details shall be clarified. Specifically, tshark, which is the console version of Wireshark, is employed to sniff the wireless medium and save the resulting RSSI values into a text file. Note that, the text file cannot be accessed within the Python code while being written. In order to resolve this issue, a shell script¹ is prepared to provide periodical operation of sniffing and recording. In particular, every 250 ms tshark processes the received packets and abstracts corresponding SNR values into the text file. In a synchronised fashion, main application reads from the text file to react in accordance with the number of delivered packets and the channel state.

Once the source codes are installed, shell script should be run first by the following command:

```
.\receive_SNR
```

Afterwards, the command given below can be used to start the main application. In accordance with this setting, communication takes place over the first channel and each message packet read from "read_it.txt" file is transmitted once. Similarly, it is possible to operate over other channels, transmit different contended packets and add repetition to each frame by making appropriate changes within text file and command line.

```
.\TriMod.py --interface=eth0 --freq=2.412e9 --repetition=1 --from-file="read_it.txt"
```

¹ The shell script is also included within the source file in [76].